Efficient Reduced Kalman Filtering and Application to Altimetric Data Assimilation in Tropical Pacific

Ibrahim Hoteit, Dinh-Tuan Pham, Jacques Blum

INRIA

INSTITUT NATIONAL DE RECHERCHE EN INFORMATIQUE ET EN AUTOMATIQUE

Efficient Reduced Kalman Filtering and Application to Altimetric Data Assimilation in Tropical Pacific

Ibrahim Hoteit, Dinh-Tuan Pham and Jacques Blum

No 3937

Mai 2000

THÈME 4

ISSN 0249-6399 ISRN INRIA/RR--3937--FR+ENG

Efficient Reduced Kalman Filtering and Application to Altimetric Data Assimilation in Tropical Pacific

Ibrahim Hoteit, Dinh-Tuan Pham and Jacques Blum

Thème 4 — Simulation et optimisation
de systèmes complexes
Projet IDOPT

Rapport de recherche n ° 3937 — Mai 2000 — 41 pages

Abstract: Several studies have demonstrated the effectiveness of the Singular Evolutive Extended Kalman (SEEK) filter and its interpolated variant called SEIK in their capacity to assimilate altimetric data into ocean models. However, these filters remain expensive for real operational assimilation. The purpose of this paper is to develop degraded forms of the SEIK filter which are less costly and yet perform reasonably well. Our approach essentially consists in simplifying the evolution of the correction basis of the SEIK filter, which is the most expensive part of this filter. To deal with model unstabilities, we also introduce two adaptive tuning schemes based on the correction basis evolution and the use of a variable forgetting factor. The filters have been implemented in a realistic setting of the OPA model over the tropical pacific zone and their performance studied through twin experiments in which the observations are taken to be synthetic altimeter data sampled on the sea surface. The SEIK filter is used as a reference for comparison. Our new filters perform nearly as well as the SEIK, but can be 2 to 10 times faster.

Key-words: Data assimilation. Reduced Kalman filtering. SEEK and SEIK Filters. Forgetting factor.

(Résumé : tsvp)

This work was carried out within the framework of the IDOPT project which is a joint project between INRIA, CNRS, University Joseph Fourier and INPG. The authors would like to thank Dr. Eric Blayo for interesting discussions during part of this work. Thanks are also given to Laurent Debreu and Laurent Parent for assistance with the numerical model.

Unité de recherche INRIA Rhône-Alpes
655, avenue de l'Europe, 38330 MONTBONNOT ST MARTIN (France)
Téléphone : 04 76 61 52 00 - International: +33 4 76 61 52 00
Télécopie : 04 76 61 52 52 - International: +33 4 76 61 52 52

Filtrage de Kalman Réduit Efficace et Application à l'Assimilation de Données Altimétriques dans le Tropical Pacifique

Résumé : Plusieurs études ont montré l'efficacité du filtre de Kalman étendu singulier évolutif (SEEK) et de sa variante interpolée, appelée SEIK, pour assimiler les données altimétriques dans les modèles océaniques. Cependant, ces deux filtres restent chers pour une océanographie opérationnelle. Le but de ce papier est de développer des formes dégradées du filtre SEIK qui sont moins coûteux mais relativement performants. Notre approche consiste essentiellement à simplifier l'évolution de la base de correction du filtre SEIK, qui est la partie la plus chère de ce filtre. Pour traiter les instabilités du modèle, nous introduisons aussi deux schémas adaptatifs basés sur l'évolution de la base de correction et sur l'utilisation d'un facteur d'oubli variable. Ces filtres ont été implémentés dans une configuration réaliste du modèle OPA dans l'océan tropical pacifique. Leurs performances ont été étudiées avec des experiences jumelles dans lesquelles les observations sont des données altimétriques de la surface libre de la mer. Le filtre SEIK est utilisé comme référence de comparaison. Nos nouveaux filtres sont aussi performents que le filtre SEIK, mais peuvent être de 2 à 10 fois plus rapides.

Mots-clé : Assimilation de données. Filtrage de Kalman réduits. Filtres SEIK et SEEK. Facteur d'oubli.

1 Introduction

In recent years there has been an increasing interest in operational data assimilation schemes in oceanography. The need for such schemes is emerging for the purposes of improving short and mid term weather prediction, developing climate prediction or for the specific objectives of the navies in various countries. Since occurrence satellites launching, considerable progress has been made in applying concepts and techniques from statistical estimation and optimal control theories to the problem of oceanographical data assimilation (see for example *Ghil and Manalotte-Rizzoli* [13] for a review). The major challenge for the coming year is to design operational data assimilation schemes which can be operated in conjunction with realistic ocean models, with reasonable quality, and at acceptable cost as in meteorology.

One of the most widely used statistical assimilation schemes is the extended Kalman (EK) filter which is an extension of the common Kalman filter to nonlinear models. However, the brute-force implementation of the EK filter in realistic ocean models is not possible in practice because of its prohibitive cost. To deal with this difficulty, different degraded forms of the EK filter, which basically reduce the dimension of the system through some kind of projection onto a low dimensional subspace, have been proposed [5, 7, 8, 11, 14].

With the same aim in view, the singular evolutive extended Kalman (SEEK) filter has been proposed by *Pham et al.* [22]. It essentially consists in approximating the error covariance matrix by a singular matrix which leads to making correction only in the directions for which the error is not sufficiently attenuated by the system. Such directions evolve in time according to the system dynamics. Further, *Pham* [23] introduces a variant called singular evolutive interpolated (SEIK) filter in which the linearization used in the SEEK filter is replaced by a linear interpolation as this could in less error for large deviations. These two filters have been applied in different realistic ocean frameworks with quite satisfactory results [4, 21, 22, 23, 26].

But, the above filters remain expensive in real operational assimilation since the evolution equation of their correction basis requires model integration for each basis vectors. Our aim is to reduce further their costs, we will simplify the evolution of the correction basis of these filters as this is the only way to obtain a significant reduction of cost. This results several degraded forms of the SEEK and SEIK filters which are much less costly and yet perform reasonably well. These filters generalize the fixed correction basis filter of *Brasseur et al.* [4] derived from an empirical orthogonal

function (EOF) analysis.

A number of studies have revealed rapid error growth when model unstabilities appear [10, 19, 25]. Our experiments corroborate this finding in that the performances of our filters decline mostly in the presence of unstability. To remedy to this, we introduce two adaptive tuning schemes. The first is based on the correction basis evolution and the second on the use of a variable forgetting factor.

This paper is organized as follows. The SEEK and SEIK filters are described in section 2. Section 3 introduces some new degraded forms of the SEEK and SEIK filters. Section 4 discusses two approaches to overcome model unstabilities. Finally, the performance of the new filters is illustrated in section 5 with some simulation results based on a realistic setting of the OPA model over the tropical Pacific ocean.

2 The singular evolutive Kalman filters

We shall adopt the notation proposed by *Ide et al.* [15]. Consider a physical system described by

$$X^t(t_k) = M(t_k, t_{k-1})X^t(t_{k-1}) + \eta(t_k) \tag{1}$$

where $X^t(t)$ denotes the vector representing the true state at time t, $M(t,s)$ is an operator describing the system transition from time s to time t and $\eta(t)$ is the system noise vector. At each time t_k, one observes

$$Y_k^o = H_k X^t(t_k) + \varepsilon_k \tag{2}$$

where H_k is the observational operator and ε_k is the observational noise. The noises $\eta(t_k)$ and ε_k are assumed to be independent random vectors with mean zero and covariance matrices Q_k and $\sigma^2 R_k$ (R_k will be often assumed to be the identity matrix), respectively.

The sequential data assimilation consists in the estimation of the state of the system at each observation time, using only observations up to this time. In the linear case, this problem has been solved by the well known Kalman filter. In the nonlinear case, one often linearizes the model around the current estimated state vector, which yields to the so-called EK filter (see for example *Ghil and Manalotte-Rizzoli* [13] for details).

The SEEK filter is introduced primarily to reduce the prohibitive cost of the EK filter in meteorology and oceanography data assimilation, due to the huge number (n) of the state variables. The main idea is to view the error covariance matrix as singular with a low rank $r << n$. This leads to a filter in which the errors correction is made only along certain directions parallel to a linear subspace of dimension r. These directions are those for which error is not sufficiently attenuated by the system dynamic.

This filter proceeds in two stages a part from an initialization stage. To initialize the filter, we make a long historical run of the model and take $X^a(t_0)$ as the average of the state vectors and $P^a(t_0)$ as the rank r approximation to their sample covariance matrix obtain via an EOFs analysis (see *Pham et al.* [22] for details).

1- Prediction stage: At time t_{k-1}, an estimate $X^a(t_{k-1})$ of the system state and its corresponding error covariance matrix $P^a(t_{k-1})$, in the factorized form $\sigma^2 L_{k-1} U_{k-1} L_{k-1}^T$ where L_{k-1} and U_{k-1} are of dimension $n \times r$ and $r \times r$ respectively, are available. The model (1) is used to forecast the state as

$$X^f(t_k) = M(t_k, t_{k-1}) X^a(t_{k-1}). \tag{3}$$

The forecast error covariance matrix is given by

$$P^f(t_k) = \sigma^2 L_k U_{k-1} L_k^T + Q_k \tag{4}$$

where

$$L_k = \mathbf{M}(t_k, t_{k-1}) L_{k-1} \tag{5}$$

and $\mathbf{M}(t_k, t_{k-1})$ is the gradient of $M(t_k, t_{k-1})$ evaluated at $X^a(t_{k-1})$.

2- Correction stage: The new observation Y_k^o at time t_k is used to correct the forecast according to

$$X^a(t_k) = X^f(t_k) + G_k[Y_k^o - H_k X^f(t_k)], \tag{6}$$

where G_k is the gain matrix given by

$$G_k = L_k U_k L_k^T \mathbf{H}_{k+1}^T R_{k+1}^{-1}, \tag{7}$$

with $\mathbf{H}_k$ the gradient of H_k evaluated at $X^f(t_k)$ and U_k computed from

$$U_k^{-1} = \left[U_{k-1} + (L_k^T L_k)^{-1} L_k^T Q_k L_k (L_k^T L_k)^{-1}\right]^{-1} + L_k^T \mathbf{H}_k^T R_k^{-1} \mathbf{H}_k L_k. \tag{8}$$

The corresponding filter error covariance matrix is then equal to

$$P^a(t_k) = \sigma^2 L_k U_k L_k^T. \tag{9}$$

Since equations (4) and (9) are only included for interpreting the results, the SEEK filter reduces drastically the computional cost with respect to the EK filter. However, in operational assimilation it still requires r times the cost of the numerical integration of the model, to compute the evolution of the correction basis L_k.

The SEEK filter may produce unstabilities, even divergence because of model nonlinearities as for the EK filter (see for example *Evensen* [9], *Gauthier et al.* [12]). To alleviate this problem, *Pham* [23] proposed a variant of the SEEK, called SEIK, in which linear interpolation is used instead of linearization.

The interest of this filter is double: firstly it avoids the complex computation of the gradient required by the SEEK filter. Secondly it is more robust with respect to model nonlinearities, since interpolation results in less error for large deviations than linearization. The novelty in this filter lies in the choice of its interpolating states $X_1^a(t_k), \ldots, X_I^a(t_k)$ which are drawn randomly at every filtering steps in such a manner as to represent the analysis state error by an ensemble of state vectors i.e.

$$X^a(t_k) = \frac{1}{I}\sum_{i=1}^{I} X_i^a(t_k), \tag{10}$$

$$P^a(t_k) = \frac{1}{I}\sum_{i=1}^{I} [X_i^a(t_k) - X^a(t_k)][X_i^a(t_k) - X^a(t_k)]^T. \tag{11}$$

From this point of view, this filter has some similarities to the ensemble Kalman filter introduced by *Evensen* [8]. However, in our approach, the number of the interpolating states I will be taken to be the smallest possible, equal to $r + 1$.

This filter proceeds in three stages apart from the initialization stage which is identical to that in the SEEK filter.

1- Drawing interpolating states: or *"Second order exact sampling"*

At time t_{k-1}, an analysis state $X^a(t_{k-1})$ and its corresponding error covariance matrix $P^a(t_{k-1})$, in the factorized form $\sigma^2 L_{k-1} U_{k-1} L_{k-1}^T$, are available. The

Cholesky decomposition of U_{k-1}^{-1} to $C_{k-1}C_{k-1}^T$ is performed which enables to write

$$P^a(t_{k-1}) = \sigma^2 L_{k-1}(C_{k-1}^{-1})^T \Omega_{k-1}^T \Omega_{k-1} C_{k-1}^{-1} L_{k-1}^T \tag{12}$$

where Ω_k is any $(r+1)\times r$ matrix with orthonormal columns and zero column sums. This matrix will be drawn randomly using the procedure described in Appendix A. Then one can take as interpolating states

$$X_i^a(t_{k-1}) = X^a(t_{k-1}) + \sigma\sqrt{r+1} L_{k-1}(\Omega_{k-1,i} C_{k-1}^{-1})^T, \tag{13}$$

for $1 \le i \le r+1$, where $\Omega_{k-1,i}$ denotes the i^{th} row of Ω_{k-1}. Note that formula (12) and (13) ensures that the sample covariance matrix of the state is precisely $P^a(t_{k-1})$.

2- Forecast stage: One applies the model to bring the interpolating states $X_i^a(t_{k-1})$ to $X_i^f(t_k)$. The state forecast $X^f(t_k)$ will be taken as the barycenter of the $X_i^f(t_k)$. The prediction error covariance matrix is approached by

$$P^f(t_k) \approx \frac{1}{r+1}\sum_{j=1}^{r+1}[X_i^f(t_k) - X^f(t_k)][X_i^f(t_k) - X^f(t_k)]^T + Q_k. \tag{14}$$

For later use, this matrix will be represented as

$$P^f(t_k) \approx L_k[(r+1)T^T T]^{-1} L_k^T + Q_k, \tag{15}$$

with a correction basis

$$L_k = [X_1^f(t_k) \cdots X_{r+1}^f(t_k)] \cdot T \tag{16}$$

where T is a $(r+1)\times r$ matrix with orthonormal columns and zero column sums. This property of T ensures that $T(T^T T)^{-1}T^T = I_d$ [1] so that (15) is indeed the same as (14). An appropriate choice of T is the matrix

$$T = \begin{pmatrix} 1 & & 0 \\ \vdots & \ddots & \vdots \\ 0 & & 1 \\ 0 & \cdots & 0 \end{pmatrix} - \frac{1}{r+1}\begin{pmatrix} 1 & \cdots & 1 \\ \vdots & & \vdots \\ \vdots & & \vdots \\ 1 & \cdots & 1 \end{pmatrix}. \tag{17}$$

[1] I_d is the identity matrix

3- Correction stage: As in the SEEK filter, the correction of the forecast state is done according to the formula

$$X^a(t_k) = X^f(t_k) + L_k U_k (HL)_k^T [Y_k^o - H_k X^f(t_k)] \tag{18}$$

with an analysis error covariance matrix

$$P^a(t_k) = \sigma^2 L_k U_k L_k^T \tag{19}$$

where $(HL)_k = [H_k X_1^f(t_k) \cdots H_k X_{r+1}^f(t_k)] \cdot T$ and U_k is computed from equation (8) but with $[\sigma^2(r+1)T^T T]^{-1}$ and $(HL)_k$ instead of U_{k-1} and $\mathbf{H}_k L_k$ respectively.

Observation error estimation: It is more suitable to estimate the parameter σ and not to use a fixed given value. Here, in the case $R_k = I_d$ we estimate σ^2 at time t_k by the quantity e_k^2/n_k^o where e_k^2 and n_k^o are updated recursively according to

$$e_k^2 = \rho e_{k-1}^2 + \|Y_k^o - H_k X^a(t_k)\|^2 \tag{20}$$

$$n_k^o = \rho n_{k-1}^o + \{dimension\ of\ Y_k^o\}. \tag{21}$$

The SEIK filter could performed better than the SEEK against the nonlinearities of the system equations, but with about the same cost.

3 Reduction of the cost of the SEIK filter

Our aim is to reduce the cost of the SEEK and SEIK filters. We will however consider only the SEIK filter since the other filter is similar, and seems to perform not as good (in our experiments). Thus we will propose several degraded forms of the SEIK filter which are less costly and yet perform reasonably well. Our approach consists essentially in simplifying the way the correction basis of the SEIK filter evolves which is the most expensive part of the filter.

3.1 The singular fixed extended Kalman (SFEK) filter

Motivated by the fact that most of the error estimation in numerical experiments in *Pham et al.* [22] was reduced immediately after the first correction, i.e. while the evolution of the EOF basis was not yet effective, *Brasseur et al.* [4] proposed to keep

the initial correction basis of the SEEK filter fixed in time. This can be justified by the fact that the state of the ocean evolves very slowly. Therefore, one can suppose that the transition operator of the ocean model is almost equal to identity and then write

$$\mathbf{M}(t_{k+1}, t_k) \approx I_d. \tag{22}$$

Under this approximation and the correction basis evolution equation (5), the correction basis of the SEEK filter will always remain constant equal to the initial EOF basis L_0. This filter, called singular fixed extended Kalman (SFEK), operates in two stages exactly as for the SEEK but without the evolution equation of the correction basis (5). It is thus almost $r + 1$ times faster than the SEEK filter.

The SFEK filter highly depends on the representativeness of the EOF correction basis. It gives good results when this basis represents sufficiently well the model variability. Its appeal is its very low cost, thus providing a cheap way to test the relevance of the EOF basis. Actually we find it useful to experiment with the SFEK filter to gain insight on the correction basis dimension r and the forgetting factor (see section 4.2) to be used in the SEIK filter and its variants.

3.2 The singular intermittently evolutive interpolated Kalman (SIEIK) filter

Another approach to simplify the way the correction basis of the SEIK filter evolves is to use the convergence property of the Kalman filter's error covariance matrix, namely $P^a(t_k)$ converges towards a fixed matrix when the model is linear and autonomous. Thus in the nonlinear case but nearly linear (and still autonomous), one can expect that $P^a(t_k)$ tends very quickly towards a semi-fixed mode in which it will evolve slowly, hence the correction basis of the SEIK filter will also evolve slowly. Therefore we propose, after an initialization period with the SEIK filter, to let the correction basis evolve intermittently according to two modes:

- **Fixed mode:** Keep the matrices L_k, U_k and $(HL)_k$ fixed. The drawing of the interpolating states is no longer perform. Prediction and correction steps are done as for the SFEK filter.

- **Keep up mode:** After a certain time in the fixed mode ($2 - 10$ days for example), the matrices L_k, U_k and $(HL)_k$ need to be updated. We start up again the SEIK filter to bring back these matrices to the semi-fixed mode.

More precisely, we let L_k evolve as in the SEIK filter starting with its previous (fix) value, and update U_k accordingly. Another advantage is that this mode can be very short (1 step for example).

This filter, called SIEIK, can be as stable as the SEIK filter but much less costly. For example, if one evolves the correction basis once every K filtering steps, one can easily see that the cost of the SIEIK filter is about K times less than the SEIK filter.

3.3 The singular semi-evolutive interpolated Kalman (SSEIK) filter

The main idea of this filter is to let only a few correction basis vector evolve and keep the other fixed. The basis vectors which do not evolve are taken to be those which contribute the least to the error filter representation, as this would minimize the effect of keeping them fixed.

To construct this filter we start by representing the analysis error covariance $P^a(t_{k-1}) = \sigma^2 L_{k-1} U_{k-1} L_{k-1}^T$ as

$$P^a(t_{k-1}) = \sigma^2 L_{k-1} (C_{k-1}^{-1})^T \Theta \Theta^T C_{k-1}^{-1} L_{k-1}^T \tag{23}$$

where C_{k-1} is the Cholesky decomposition of U_{k-1}^{-1} and Θ is an arbitrary orthogonal matrix. This show that there is an equivalent representation

$$P^a(t_{k-1}) = \sigma^2 \tilde{L}_{k-1} \tilde{L}_{k-1}^T \tag{24}$$

with the new correction basis

$$\tilde{L}_{k-1} = L_{k-1} (C_{k-1}^{-1})^T \Theta, \tag{25}$$

One can then split this new representation as

$$P^a(t_{k-1}) = \sigma^2 \tilde{L}_{k-1}^{r_0} \tilde{L}_{k-1}^{r_0\,T} + \sigma^2 \tilde{L}_{k-1}^{r_1} \tilde{L}_{k-1}^{r_1\,T} \tag{26}$$

where $\tilde{L}_{k-1}^{r_0}$ and $\tilde{L}_{k-1}^{r_1}$ contain the first r_0 and the last $r_1 = r - r_0$ columns of $\tilde{L}_{k-1}$ respectively. The above representation holds for any orthogonal matrix Θ, the idea is to chooses Θ in such a manner that the columns of $\tilde{L}_{k-1}$ are orthogonal and ranked according to their norm in increasing order (for some metric $\mathcal{M}$ in the state space, see section 5.2.2). In this way, the matrix $\tilde{L}_{k-1}^{r_1}$ will contribute the most to the filter error representation. Such a matrix Θ can be easily constructed as the matrix whose

columns are the eigenvectors of $C_{k-1}^{-1} L_{k-1}^T \mathcal{M} L_{k-1} C_{k-1}^{-T}$ ranked according to their eigenvalue in increasing order.

From the above considerations, we will let only the matrix $\tilde{L}_{k-1}^{r_1}$ evolve (in the same way as in the SEIK filter) while keeping the matrix $\tilde{L}_{k-1}^{r_0}$ fixed in time. Specifically, we construct the interpolating states $X_1^a(t_{k-1}), \ldots, X_{r_1+1}^a(t_{k-1})$ with barycenter $X^a(t_{k-1})$ and covariance matrix $\sigma^2 \tilde{L}_{k-1}^{r_1} \tilde{L}_{k-1}^{r_1\,T}$ and let $\check{L}_{k-1}$ be the matrix $[\tilde{L}_{k-1}^{r_0}, [X_1^a(t_{k-1}) \cdots X_{r_1+1}^a(t_{k-1})]T]$ where T is as in (17) with r_1 instead of r. By this construction, we can write

$$P^a(t_{k-1}) = \sigma^2 \check{L}_{k-1} \begin{bmatrix} I_d & 0 \\ 0 & \sigma^2(r_1+1)T^T T \end{bmatrix}^{-1} \check{L}_{k-1}^T. \tag{27}$$

Then in the forecast stage we compute the r_1 interpolating states $X_i^f(t_k)$ by applying the model on $X_i^a(t_{k-1})$ and approximate the forecast error covariance matrix by

$$P^f(t_k) = \sigma^2 \tilde{L}_{k-1}^{r_0} \tilde{L}_{k-1}^{r_0\,T} + \frac{1}{r_1+1} \sum_{i=1}^{r_1+1} [X_i^f(t_k) - X^f(t_k)][X_i^f(t_k) - X^f(t_k)]^T + Q_k. \tag{28}$$

Again, the above matrix can be rewritten as

$$P^f(t_k) = \sigma^2 \check{L}_k \begin{bmatrix} I_d & 0 \\ 0 & \sigma^2(r_1+1)T^T T \end{bmatrix}^{-1} \check{L}_k^T + Q_k \tag{29}$$

where $X_i^f(t_k) = M(t_k, t_{k-1}) X_i^a(t_{k-1})$ for $i = 1, ..., r_1+1$, $X^f(t_k)$ is the barycenter of the $X_i^f(t_k)$ and $\check{L}_k = [\tilde{L}_{k-1}^{r_0}, [X_1^f(t_k) \cdots X_{r_1}^f(t_k)]T]$.

This representation is the same as (4) in the SEEK filter but with U_{k-1} replaced by the matrix

$$\begin{bmatrix} I_d & 0 \\ 0 & \sigma^2(r_1+1)T^T T \end{bmatrix}. \tag{30}$$

Therefore one may apply the same correction step as in the SEEK filter to get U_k and hence $P^a(t_k)$.

The cost of the SSEIK filter is about $(r+1)/(r_1+1)$ times the SEIK filter. Moreover, since the value of r_1 can be taken equal to 1 or 2, this filter is much less expensive than the SEIK filter.

3.4 Doubling the basis of the SEIK filter

Consider a physical system described by the differential equation

$$\frac{dX}{dt} = F(X(t), t), \tag{31}$$

which is quasi-autonome in the sens that the gradient of $F(\cdot, t)$ is independent of t. Let $\mathbf{F}(\cdot)$ denote this gradient and $M(t_{k+1}, t_k)$ be the transition operator from time t_k to t_{k+1}, associated with the system (31).

Recall that in the SEEK filter, the i^{th} column $L_{k,i}$ of the correction basis L_k evolves according to the equation

$$L_{k+1,i} = \mathbf{M}(t_{k+1}, t_k) L_{k,i} \tag{32}$$

where $\mathbf{M}(t_{k+1}, t_k)$ is the gradient of $M(t_{k+1}, t_k)$ evaluated at $X^a(t_k)$. This gradient is such that the vector function $v(t) = \mathbf{M}(t, t_k) L_{k,i}$ is a solution of the differential system

$$\left\{ \begin{array}{lcl} dv/dt & = & \mathbf{F}(X^a(t))v(t) \\ v(t_k) & = & L_{k,i}. \end{array} \right. \tag{33}$$

Let $v_h(t) = v(t+h)$, we have

$$\frac{d(v_h - v)/h}{dt} = \frac{\mathbf{F}(X^a(t+h)) - \mathbf{F}(X^a(t))}{h} v_h(t) + \mathbf{F}(X^a(t)) \frac{v_h(t) - v(t)}{h}.$$

If the model is almost linear then the first term in the right hand side of the above equation may be negligible compared to the second term. Thus the limit $\mathbf{v}$ of $(v_h - v)/h$ as h tends to zero verifies

$$\frac{d\mathbf{v}}{dt} \approx \mathbf{F}(X^a(t_k))\mathbf{v}. \tag{34}$$

Since, by construction, $\mathbf{v}(t_k)$ and $\mathbf{v}(t_{k+1})$ are no other than $\mathbf{F}(X^a(t_k))L_{k,i}$ and $\mathbf{F}(X^a(t_{k+1}))L_{k+1,i}$ respectively, the above equation is equivalent to

$$\mathbf{F}(X^a(t_{k+1}))L_{k+1,i} \approx \mathbf{M}(t_{k+1}, t_k)\mathbf{F}(X^a(t_k))L_{k,i}. \tag{35}$$

One recognizes in the last formula the evolution equation of the correction basis vectors (32), with $\mathbf{F}(X^a(t_.))L_{.,i}$ in place of $L_{.,i}$. Therefore, if $\mathbf{F}(X^a(t_k))L_{k,i}$ was a

basis correction vector at time t_k then $\mathbf{F}(X^a(t_{k+1}))L_{k+1,i}$ is too at time t_{k+1}. This remark enables us to "double" the dimension of the correction basis of the SEEK filter without really increasing the computation cost. Indeed, if one initializes the correction basis by

$$\tilde{L}_0 = \Big[L_{0,1} \cdots L_{0,r} \ \vdots \ \mathbf{F}(X^a(t_0))L_{0,1} \cdots \mathbf{F}(X^a(t_0))L_{0,r} \Big], \tag{36}$$

the correction basis at time t_k can be approximated by

$$\tilde{L}_k = \Big[L_{k,1} \cdots L_{k,r} \ \vdots \ \mathbf{F}(X^a(t_k))L_{k,1} \cdots \mathbf{F}(X^a(t_k))L_{k,r} \Big]. \tag{37}$$

Thus to compute the new correction basis $\tilde{L}_k$ at time t_k, one has just to compute its first r columns and than to deduce the last r columns via the post multiplication of the first one by the matrix $\mathbf{F}(X^a(t_k))$.

We develop now the SEIK version of this filter, call singular double basis evolutive interpolated Kalman (SDEIK) filter. It consists of three stages apart of an initialization stage, as in the SEIK filter.

1- Drawing interpolating states: It will be seen later that at the beginning of the $(k-1)-th$ step, one has a decomposition of the analysis error covariance matrix in the form

$$P^a(t_{k-1}) = \sigma^2 \bar{L}_{k-1} \bar{U}_{k-1} \bar{L}_{k-1}^T, \tag{38}$$

where

$$\bar{L}_{k-1} = \Big[[X_1^f(t_{k-1}) \cdots X_{r+1}^f(t_{k-1})]T \ \vdots \ [\dot{X}_1^f(t_{k-1}) \cdots \dot{X}_{r+1}^f(t_{k-1})]T \Big], \tag{39}$$

with $\dot{X}_i^f(t_{k-1})$ being $F(X_i^f(t_{k-1}), t_{k-1})$ and $\bar{U}_{k-1}$ is a $2r \times 2r$ matrix. Further the analysis vector $X^a(t_{k-1})$ is also available as a linear combination of $X_1^f(t_{k-1}), \ldots, X_{r+1}^f(t_{k-1})$.

Decompose the $r \times r$ upper left corner U_{k-1}^{-1} of $\bar{U}_{k-1}^{-1}$ into $C_{k-1}C_{k-1}^T$ and draw a random matrix Ω_{k-1} as in the SEIK filter. One can then represent $P^a(t_{k-1})$ as

$$\begin{aligned} P^a(t_{k-1}) \ = \ & \bar{L}_{k-1} \begin{bmatrix} (\Omega_{k-1}C_{k-1}^{-1})^T T & 0 \\ 0 & (\Omega_{k-1}C_{k-1}^{-1})^T T \end{bmatrix} (r+1)\sigma^2 \tilde{U}_{k-1} \\ & \begin{bmatrix} T^T(\Omega_{k-1}C_{k-1}^{-1}) & 0 \\ 0 & T^T(\Omega_{k-1}C_{k-1}^{-1}) \end{bmatrix} \bar{L}_{k-1}^T, \end{aligned} \tag{40}$$

where

$$\tilde{U}_{k-1}^{-1} = (r+1)\begin{bmatrix} T^T(\Omega_k C_{k-1}^{-1}) & 0 \\ 0 & T^T(\Omega_k C_{k-1}^{-1}) \end{bmatrix} \bar{U}_{k-1}^{-1}\begin{bmatrix} (\Omega_{k-1}C_{k-1}^{-1})^T T & 0 \\ 0 & (\Omega_{k-1}C_{k-1}^{-1})^T T \end{bmatrix}. \quad (41)$$

Noting that the $r \times r$ upper left corner matrix of $\tilde{U}_{k-1}$ is the matrix $(r+1)T^TT$, the analysis interpolating states $X_i^a(t_{k-1})$ can then be constructed as in the SEIK filter by the formula (13) in which L_{k-1} is the matrix that contains the first r columns of $\bar{L}_{k-1}$.

Since $L_{k-1}(\Omega_{k-1}C_{k-1}^{-1})^T = [X_1^f(t_{k-1}) \cdots X_{r+1}^f(t_{k-1})]T(\Omega_{k-1}C_{k-1}^{-1})^T$, the formula (13) shows that $X_i^a(t_{k-1})$ is a linear combination of $X_1^f(t_{k-1})$, ..., $X_{r+1}^f(t_{k-1})$. Further, since each column of T has its elements summing to zero, the coefficient of this linear combination sum to 1. By approximating the function $F(\cdot, t_{k-1})$ by its linear interpolation based on $X_1^f(t_{k-1})$, ..., $X_{r+1}^f(t_{k-1})$ the vectors $\dot{X}_i^a(t_{k-1}) = F(X_i^a(t_{k-1}), t_{k-1})$ can also be written as linear combinations of $X_1^f(t_{k-1})$, ..., $X_{r+1}^f(t_{k-1})$ with the same coefficients as those for $X_i^a(t_{k-1})$. Consequently, we have

$$P^a(t_{k-1}) \approx \left[[X_1^a(t_{k-1}) \cdots X_{r+1}^a(t_{k-1})]T \ \vdots \ [\dot{X}_1^a(t_{k-1}) \cdots \dot{X}_{r+1}^a(t_{k-1})]T \right] \sigma^2 \tilde{U}_{k-1}^{-1} \left[[X_1^a(t_{k-1}) \cdots X_{r+1}^a(t_{k-1})]T \ \vdots \ [\dot{X}_1^a(t_{k-1}) \cdots \dot{X}_{r+1}^a(t_{k-1})]T \right]^T. \quad (42)$$

2- Forecast stage: The state forecast $X^f(t_k)$ is taken as the barycenter of $X_1^f(t_{k-1})$, ..., $X_{r+1}^f(t_{k-1})$ with the prediction error covariance matrix

$$P^f(t_k) = \bar{L}_k \tilde{U}_{k-1} \bar{L}_k^T + Q_k, \quad (43)$$

where the new correction basis is now given by

$$\bar{L}_k = \left[[X_1^f(t_k) \cdots X_{r+1}^f(t_k)]T \ \vdots \ [\dot{X}_1^f(t_k) \cdots \dot{X}_{r+1}^f(t_k)]T \right]. \quad (44)$$

3- Correction stage: One computes

$$\bar{U}_k^{-1} = \sigma^2 \tilde{U}_{k-1}^{-1} + (H\bar{L})_k^T R_k^{-1} (H\bar{L})_k, \quad (45)$$

than corrects the prediction vector by

$$X^a(t_k) = X^f(t_k) + \bar{L}_k\bar{U}_k(H\bar{L})_k^T[Y_k^o - H_kX^f(t_k)]. \tag{46}$$

Thus the analysis vector $X^a(t_k)$ is a linear combination of $X_1^f(t_k), \ldots, X_{r+1}^f(t_k)$, as it has been announced earlier. The corresponding analysis error covariance matrix is

$$P^a(t_k) = \sigma^2\bar{L}_k\bar{U}_k\bar{L}_k^T, \tag{47}$$

which is also of the form announced earlier.

Numerical computation of $\dot{X}_i^f(t_k)$: One can use the time differencing Euler scheme of the system (31) to compute

$$F(X(t_k), t_k) = \frac{1}{\delta}\Big[M(t_k+\delta, t_k)X(t_k) - X(t_k)\Big], \tag{48}$$

where δ is the time step of the numerical model.

4 Tracking model unstabilities

A large number of studies have made clear that rapid error growth in periods of baroclinic and barotropic unstability is nonmodal [10, 19, 25]. *Cohn et al.* [6] noted that all their degraded EK filters failed to capture the unstability, and generally diverge. The degraded forms of the SEIK filter presented in section 3 can not be an exception to this observation since the assumptions on which we have constructed them are no more justified in unstable periods. To remedy this, we introduce two adaptive tuning schemes: the first on the correction basis evolution and the second on the forgetting factor.

4.1 Adaptive tuning of the correction basis evolution

In our experiments we noticed that the SEIK filter is more or less well-behaved in the presence of unstability. This motivates letting the correction basis evolve with a degraded SEIK filter when the model is stable and with the SEIK filter when the model is unstable.

To detect the periods of model unstability, one can track the filter's state by computing an instantaneous term average and a long average of the prediction error norm, denoted by s_k and l_k respectively. If $s_k \leq l_k$, one may assume that steady conditions have been achieved and consider that the model is in a stable period. In this case we let the correction basis evolve according to a degraded SEIK filter. If $s_k > l_k$ this is an indication that the model may be in an unstable period, therefore it is better to use the SEIK's evolution equation for the correction basis.

The estimates of s_k and l_k are computed recursively as follows

$$s_k = \alpha s_{k-1} + (1-\alpha) * \|Y_k^o - H_k X^f(t_k)\|, \quad (49)$$

$$l_k = \beta l_{k-1} + (1-\beta) * \|Y_k^o - H_k X^f(t_k)\| \quad (50)$$

where α and β are constants chosen such that $\beta \lesssim 1$ and $\alpha < \beta$.

4.2 Adaptive tuning of the forgetting factor

There are three reasons behind the use of the forgetting factor in the SEIK filter (and the SEEK filter). Firstly, it limits the effective filter memory length by discarding old data. This will attenuate the error propagation and enable the SEIK filter to follow system changes. Secondly, it sets up the gain matrix to avoid the "blow up" phenomena (see *Aström* [2]). Thirdly, it does not require any extra cost for its implementation: the filter remain unchanged except for the emergence of the forgetting factor ρ in the time propagation error covariance equation (see *Pham* [23]). Specifically, the updating equation for U_k now changes to

$$U_k^{-1} = \left[\rho\sigma^2(r+1)T^TT]^{-1} + (L_k^TL_k)^{-1}L_kQ_kL_k(L_k^TL_k)^{-1}\right]^{-1} + (HL)_k^TR_k^{-1}(HL)_k. \quad (51)$$

With $\rho = 1$, all data have the same weight, but with $\rho < 1$, recent data are exponentially more weighted than old data.

However, the use of a too small forgetting factor when the system evolution is stable would degraded the filter performance especially when there is little information in the measurements. To maximize the benefit of the forgetting factor, we propose to use a variable one (*Sorenson and Sacks* [24]): such factor should be close to 1 when the model is stable and much less then 1 when the model is unstable. Indeed, old data should be forgotten more in the last case to adapt the filter to the

new model's mode. Therefore, we will give the forgetting factor the value ρ_1^* or ρ_2^* according to the relative magnitudes of the instantaneous and the long-term and prediction error s_k and l_k, i.e.

$$\rho_k = \begin{cases} \rho_1^* \lesssim 1 & \text{if} \quad c * s_k < l_k, \\ \rho_2^* < \rho_1^* & \text{if} \quad c * s_k \geq l_k. \end{cases}$$

where c is a tuning constant.

Note that our two adaptive schemes are tuned according to the same quantities s_k and l_k, one can then use the adaptive scheme on the forgetting factor together with the adaptive scheme on the correction basis evolution.

5 Application to altimetric data assimilation in the OPA model of the tropical Pacific

In order to evaluate the performance of the degraded SEIK filters, we have implemented them in a realistic setting of the OPA model in the tropical Pacific ocean, under the assumption of a perfect model ($Q_k = 0$). The assimilation is based on the pseudo-observations which are extracted from twin experiments. The SEIK filter is used as a reference to compare the performance of these new filters. The configuration and the characteristics of the model used in our experiments are presented in the next section.

5.1 OPA model in tropical Pacific

In this section we briefly present the model basics and a description of our configuration.

5.1.1 Model description

The OPA model (OPA for Océan PArallélisé) is a primitive equation ocean general circulation model which has been developed at the LODYC laboratory (Laboratoire d'Océanographie DYnamique et de Climatologie) to study large scale ocean circulation. It solves the Navier-Stokes equations which express the momentum balance, the hydrostatic equilibrium, the incompressibility, the heat and salt balance and a non-linear realistic equation of state plus the rigid lid assumption and some hypothesis made from scale considerations. The system equations is written in curvilinear

z-coordinates and discretized using the centered second order finite difference approximation on a three dimension generalized "C-grid Arakawa". In this scheme, the scalar variables are computed in the center of the cells and the vector variable in the center of cell faces (see *Arakawa* [1] for details). Time stepping is achieved by two time differencing schemes: a basic leap-frog scheme associated to an Asselin filter for the non-diffusive processes and a forward scheme for diffusive terms. The sub-grid scale physics are a tracer diffusive operators of second order on the vertical, the eddy coefficients being computed from a turbulent closure model (see *Blanke and Delecluse* [3]). On the lateral, diffusive and vicious operators can be either of second or of fourth order. The reader is referred to the OPA reference manual *Madec et al.* [18] for more details.

5.1.2 Model configuration

The model domain covers the entire tropical Pacific basin extending from $120°E$ to $70°O$ and from $33°S$ to $33°N$ and the level depth varies from 0 at the sea surface to $4000m$. The number of horizontal grid points is 171×59 on 25 vertical levels. The model equations are solved on an isotropical horizontal grid with a maximal resolution at the equator ($0.5°$) and goes down to $2°$ to north and south boundaries. The vertical resolution is approximatively $10m$ from the sea surface to $120m$ depth then decreases to $1000m$ at the sea bottom. The time step is one hour.

The bathymetry is relatively coarse. It was obtained from Levitus data's mask [17]. The forcing fields are interpolating from the ECMWF (European center for medium-range weather forecasts) reanalysis with monthly variability. It is composed of wind stress and heat, temperature and fresh water fluxes. Zero fluxes of heat and salt and non-slip conditions are applied at solid boundaries.

A second order horizontal friction and diffusion scheme for momentum and tracers is chosen with a coefficient of $2000m^2/s$ in the strip $10°N - 10°S$ and increase up to $10000m^2/s$ at the north and south basins boundaries. The static unstabilities are resolved in the turbulent closure scheme.

The model starts from rest (i.e. with zero velocity field) and S and T are stem from seasonal climatologic Levitus data [17].

5.2 Experiments design

5.2.1 The state vector

The state vector is the set of prognostic model variables that must be initialized independently. Since the prognostic variables of the OPA model are the zonal U and meridional V velocities, the salinity S and the temperature T, one should consider the state vector

$$X^t = (U , V , S , T)^T. \tag{52}$$

However, the observed variable, which is the sea surface height SSH, is a diagnostic variable computed from the barotrope velocity by a complex nonlinear algebraic equation. Thus, the observation operator H which relies the observed variable to this state vector will be nonlinear. Moreover, in order to determine H one should inverse this equation and this can be very costly. To avoid these difficulties, we will adopt a pseudo-state vector in our experiments which contains the true state vector augmented by the SSH, namely

$$X^t = (U , V , S , T , SSH)^T. \tag{53}$$

In this case, H will always be linear of the form $(0 \vdots I_d)$. Of course, the dimension of the state vector will increase but the increase is insignificant since the SSH is computed only on the sea surface. More precisely, the number of state variable is now $4 \times 171 \times 59 \times 25 + 171 \times 59 = 1\,018\,989$ instead of $4 \times 171 \times 59 \times 25 = 1\,008\,900$.

5.2.2 Filters initialization

Following the strategy explained in *Pham et al.* [22], the choice of the initial state estimator flow field and the corresponding error covariance matrix is made through a simulation of the model itself. Note that this is only done once, and the results can be used to initialize all our degraded SEIK filters. In the present study, the data for the assimilation experiments is again simulated but in an unrelated way with the above simulation.

Thus, in a first experiment, the model has been spun up for 7 years from 1980 to 1986 with the aim to reach a statistically steady state of mesoscale turbulence. Next, another integration of 4 years is carried out from 1987 to 1990 to generate a historical sequence H_S of model realization. A sequence of 480 state vectors was retained by storing 1 state vector every 3 days to reduce the calculation since successive states

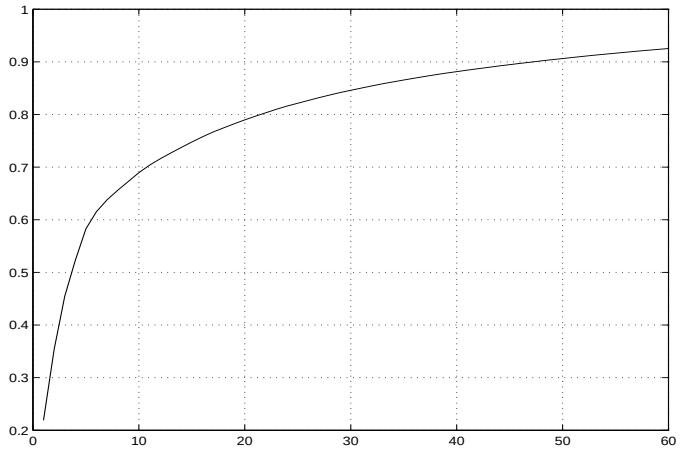

Figure 1: percentage of inertia versus the number of retained EOFs.

are quite similar. Because the state variables in (53) are not of the same nature, we shall in fact apply a multivariate EOFs analysis. We define a metric $\mathcal{M}$ in the state space to make distance between state vectors independent from unit of measure. We choose $\mathcal{M}$ as the diagonal matrix with diagonal elements being the spatial variances of each state variables, namely U, V, S, T and SSH, average over the grid points. The initial error covariance matrix $P^a(t_0)$ is then estimated via an EOFs analysis on the sample H_S (*Pham et al.* [22]).

Figure 1 plots the number of EOFs and the percentage of variability (or inertia) contained in the sample H_S they explain. From this result, we have chosen to retain $r = 30$ EOFs in all assimilation experiments, as this achieve 85% of the inertia of the sample and this percentage is not much increased for higher value of r.

5.2.3 Data and filters validation

Twin experiments are used to assess the performances and the capabilities of our filters. A reference experiment is performed and the reference X^t retained to be latter compared with the fields produced during the assimilation experiments. More precisely, a sequence of 250 state vectors was retained every $24h$ during the period of Mars 1^{st} 1991 to October 10^{st} 1991.

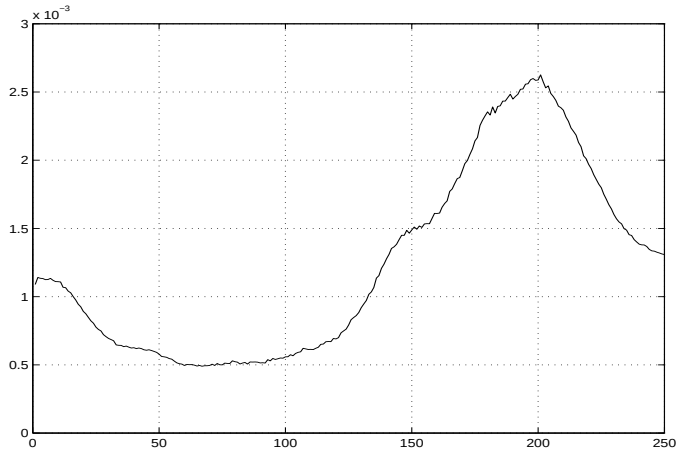

Figure 2: Relative variation of the state vector.

The assimilation experiments are performed using the pseudo-measurements which are extracted from the reference experiment. The SSH are assumed to be observed at every grid points of the model surface with a nominal accuracy of $3cm$. The observation error is simulated by adding randomly generated Gaussian noise to the synthetic observations of SSH. Note that in the assimilation interval, a period of very strong model unstability occur between July and September (see Figure 2).

Finally, the performance of all our filters is evaluated by comparing the relative root mean square ($RRMS$) error for each state variable, in each layer or in the whole domain of the ocean model. The $RRMS$ is defined as

$$RRMS(t_k) = \frac{\|X^t(t_k) - X^a(t_k)\|}{\|X^t(t_k) - \bar{X}\|}, \tag{54}$$

where $\bar{X}$ is the mean state of the sample H_S and $\|\cdot\|$ denotes the Euclidien norm. Note that the error is relative to the free-run error since the denominator represents the error when there is no observation and the analysis vector is simply taken as the mean state vector.

5.3 Results of assimilation experiments

We first present the results of the SEIK filter and compare them to those of the SEEK filter. Next, we implement the degraded SEIK filters to study their performances with respect to the SEIK filter. Finally, we investigate the effect of our two adaptive tuning schemes presented in section 4 on the performance of our filters.

- *SEIK and SEEK filters*

The SEIK filter has been implemented with a fixed forgetting factor equal to $\rho = 0.8$. It can be seen from Figure 3-7 that the it performs very well both in the upper layers and in the lower layers. Although its performance appears to degrade somewhat in the presence of unstability, the filter behaves satisfactory during this period. It may appear that the meridional velocity V is not sufficiently well-assimilated because the assimilation error is only reduced to almost a half. However, since the velocity field of the tropical Pacific ocean is essentially zonal, the meridional velocity fields generally, and especially our reference field at time Mars 1^{st} 1991, are well-approached by the average meridional velocity. This implies that our initial error is already low and therefore it would be hard to reduce it much further.

The results of our experiments for the SEIK filter have been presented in both the upper and lower layers for completeness, but we have noticed that the difference between our new filters and the SEIK filter, in term of their $RRMS$ are quite similar the upper lower layer. Therefore, in the sequel we will only present global results for all layers.

We have also conducted a preliminary experiment with the SEEK filter, which confirm the advantage of the interpolation in the SEIK filter over the linearization used in the SEEK filter. Figure 8 plots the assimilation results of these two filters using the same setup as before. Clearly the SEIK filter performs better, particularly with regard to the velocity components U and V, in the unstable period. The SEIK filter thus seems to be more robust than the SEEK filter, in the sens that it can support more deviation from linearity without being broken down. Therefore in the sequel we will be interested only in the variants of the SEIK filter and shall evaluate their performance against this filter.

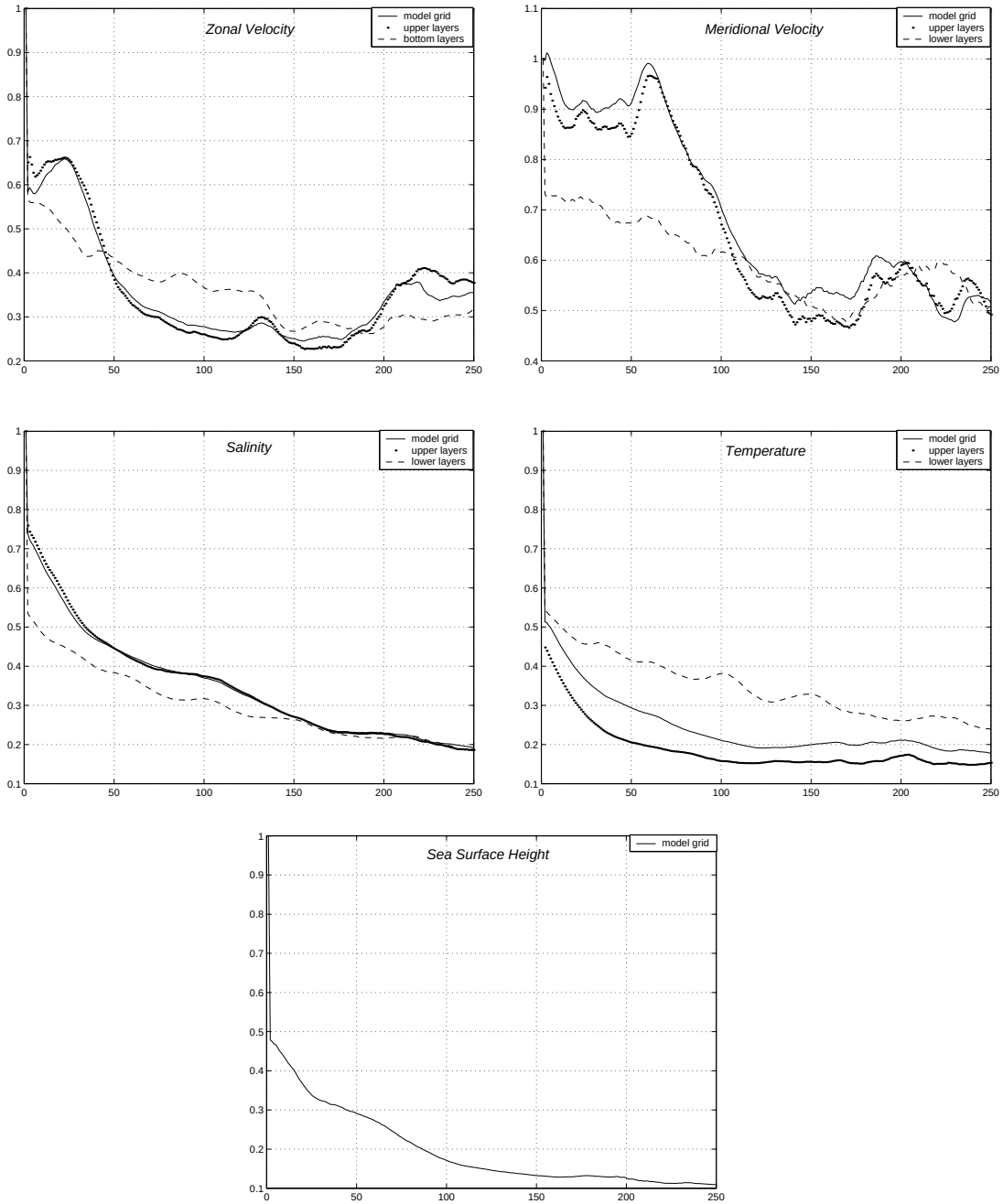

Figure 3: Evolution in time of the $RRMS$ for the SEIK filter on the whole model grid and on the (mean of the 5) upper and the (mean of the 5) lower layers.

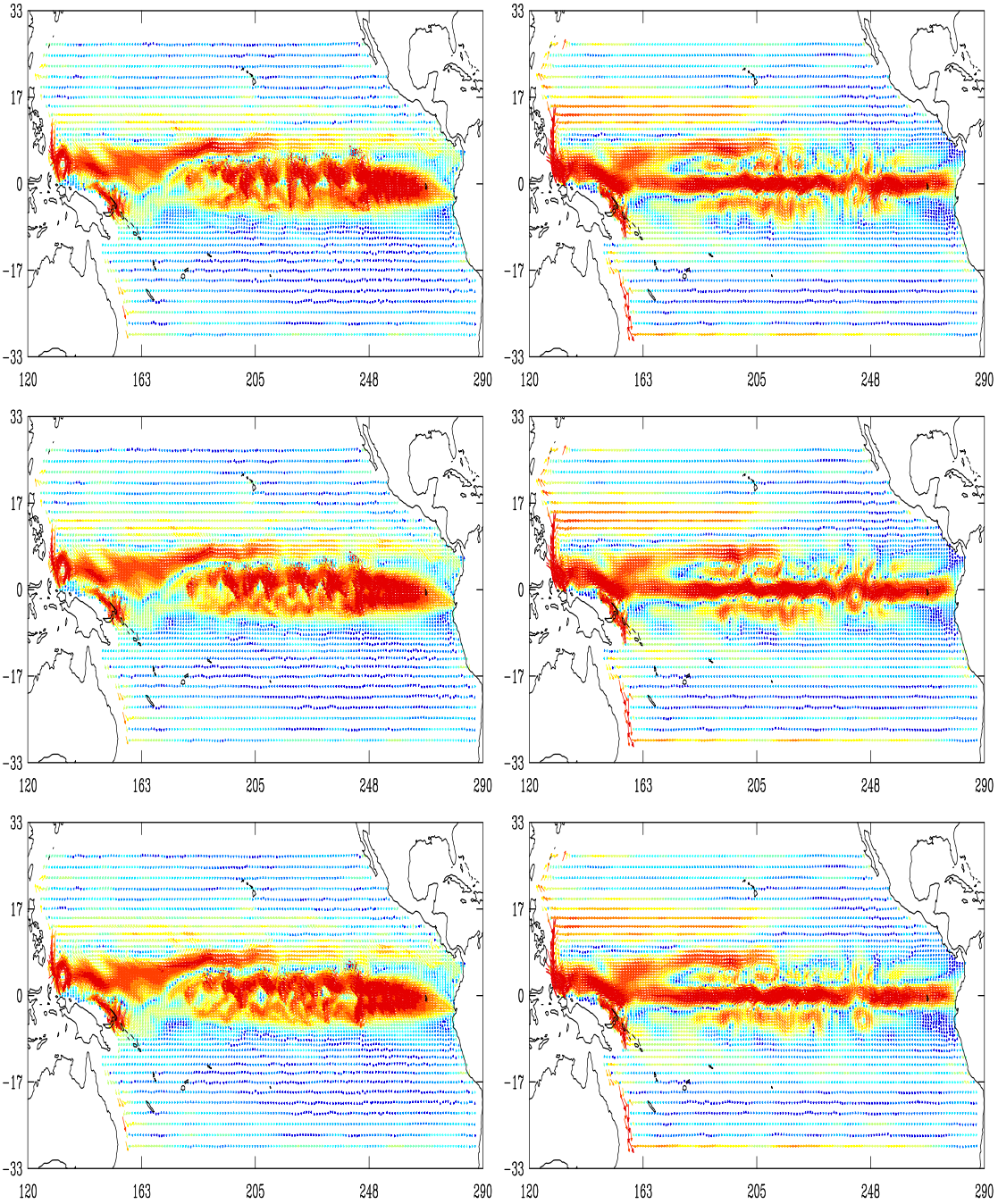

Figure 4: Maps of ocean velocity on Sept 1^{st} 90 in the first (left) and the 17^{th} (right) layers: from the SEIK filter (top); reference (middle); from the SEEK filter (bottom).

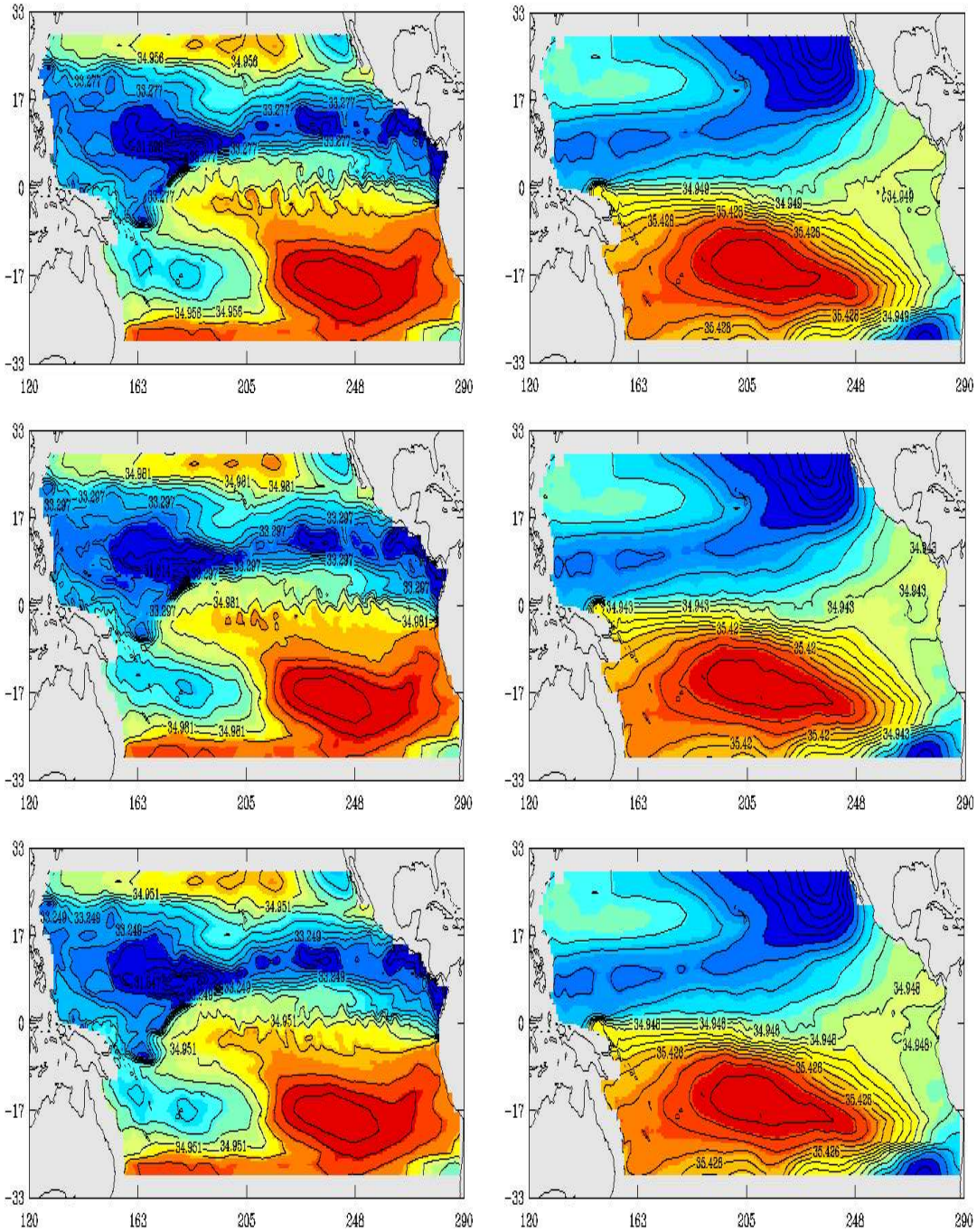

Figure 5: Maps of sea salinity on Sept 1^{st} 90 in the first (left) and the 17^{th} (right) layers: from the SEIK filter (top); reference (middle); from the SEEK filter (bottom).

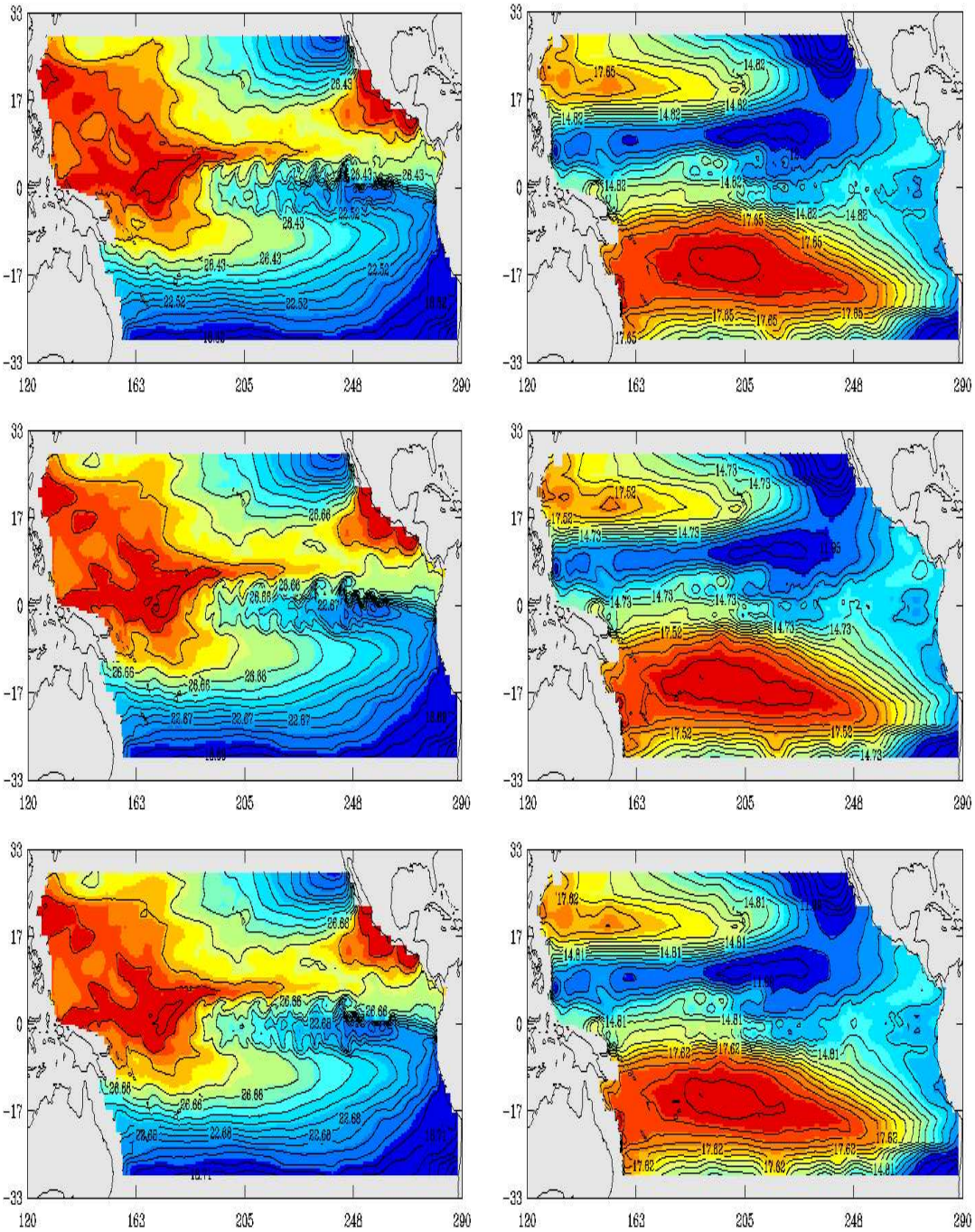

Figure 6: Maps of sea temperature on Sept 1^{st} 90 in the first (left) and the 17^{th} (right) layers: from the SEIK filter (top); reference (middle); from the SEEK filter (bottom).

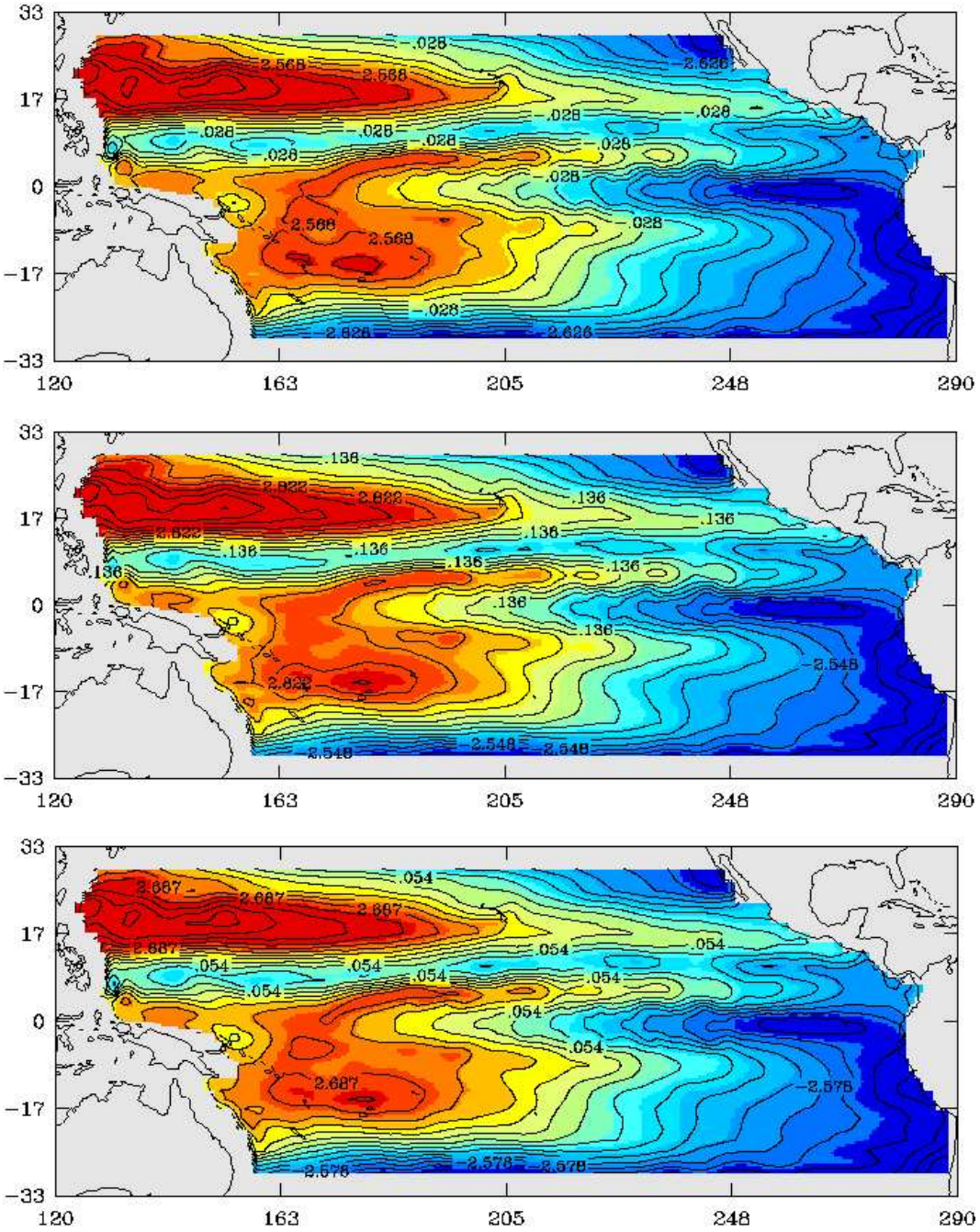

Figure 7: Maps of sea surface pressure on Sept 1^{st} 90: from the SEIK filter (top); reference (middle); from the SEEK filter (bottom).

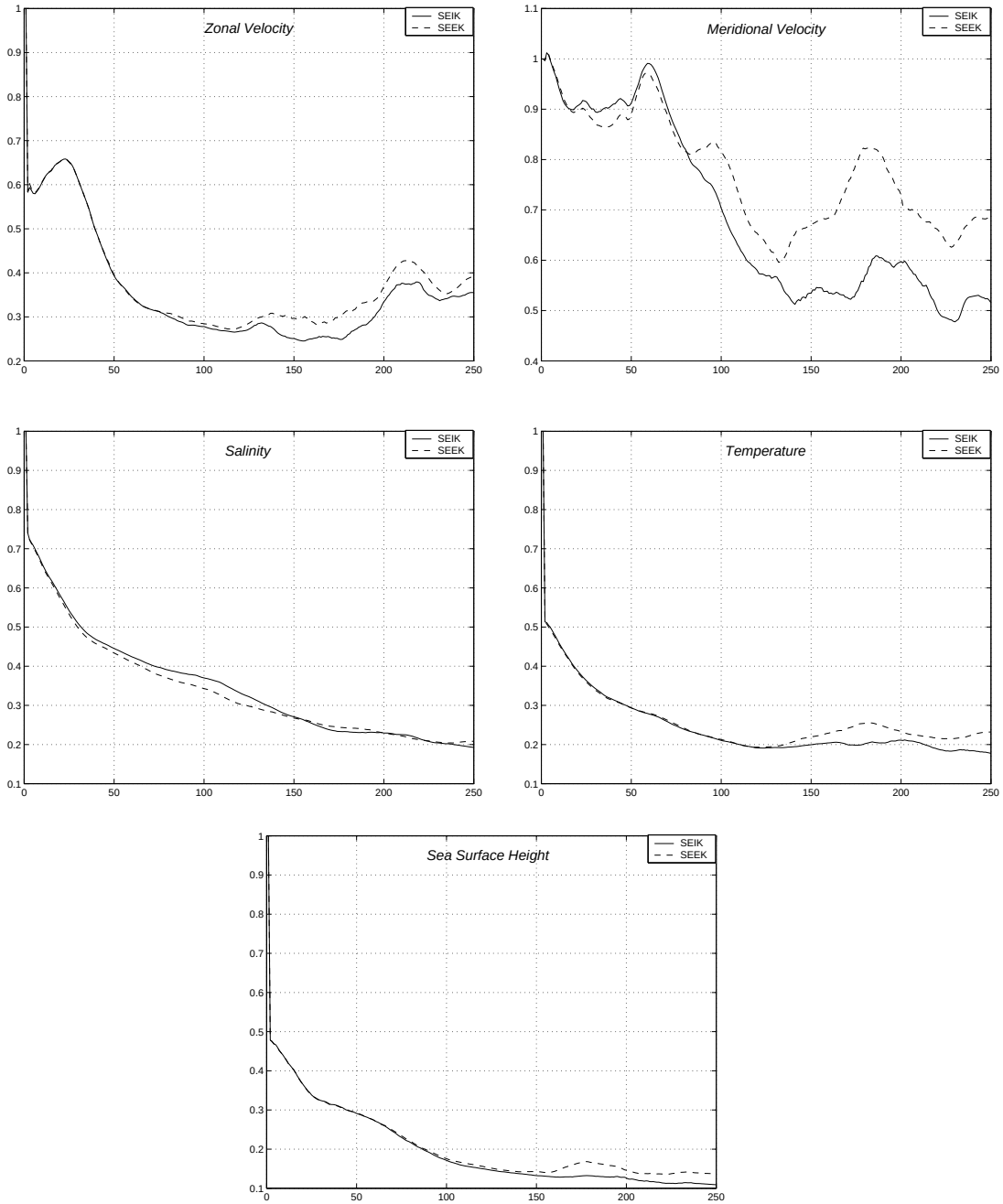

Figure 8: Evolution in time of the $RRMS$ for the SEIK and SEEK filters.

• *Degraded SEIK filters*

In order to study the numerical performance of the degraded SEIK filters with respect to the SEIK filter, we have implemented them under the same previous setup. For the SSEIK filter, only one vector out of 30 of the correction basis evolves. For the SIEIK filter, the whole basis of 30 vectors was to evolve once every two filtering steps after an initialization period of 10 steps (using the SEIK filter). Concerning the SDEIK filter, an evolutive basis of 15 vectors was "doubled" as in (44) to yield a basis of 30 vectors. Thus, the SFEK, SSEIK, SIEIK and the SDEIK filters are respectively about 30, 15, 2 and 2 times faster than the SEIK filter (Appendix B provides a summary table of the cost for all filtering schemes used below with respect to the SEIK's cost). Results of the experiments are plotted in Figure 9.

The SFEK filter is relatively well-behaved in a stable period. Its performance degrades when model unstability appears. This suggests that the EOFs analysis has failed to capture a large part of the ocean variability, particularly those occurring in the unstable periods. Indeed the performance of this filter depends highly on the representativeness of the correction basis obtained from the EOF analysis.

The results of the SIEIK filter are very encouraging. It seems to be reasonably well-behaved in the unstable period thanks to the update of the correction basis. The good performance of this filter seems to suggests the existence of the semi-fixed mode for an autonomous nearly-linear model. We have also noticed, in other experiences not presented here, that the results of this filter depend mostly on the fixed and the keep up modes length noted K_f and K_u respectively. Its performance is a decrease function of K_f and an increased function of K_u, as one would expect.

Concerning the results of the SSEIK filter, it performs very well in the stable period. However, its performances degrades quickly during the unstable period.

Finally, with regard to the results of the SDEIK filter which are in some way a bit disappointing, we have started this filter by using the SEIK to let the correction basis settle into a "more stable" mode. Despite a very good behavior in the stable period, this filter diverges some what, especially in the upper layers, during the unstable period (see Figure 10). The poor performance of the SDEIK filter on the upper layers let us presume that it is very sensible to the forcing fields. Note that the results of this experiment was plotted together with the results of the SDEIK filter

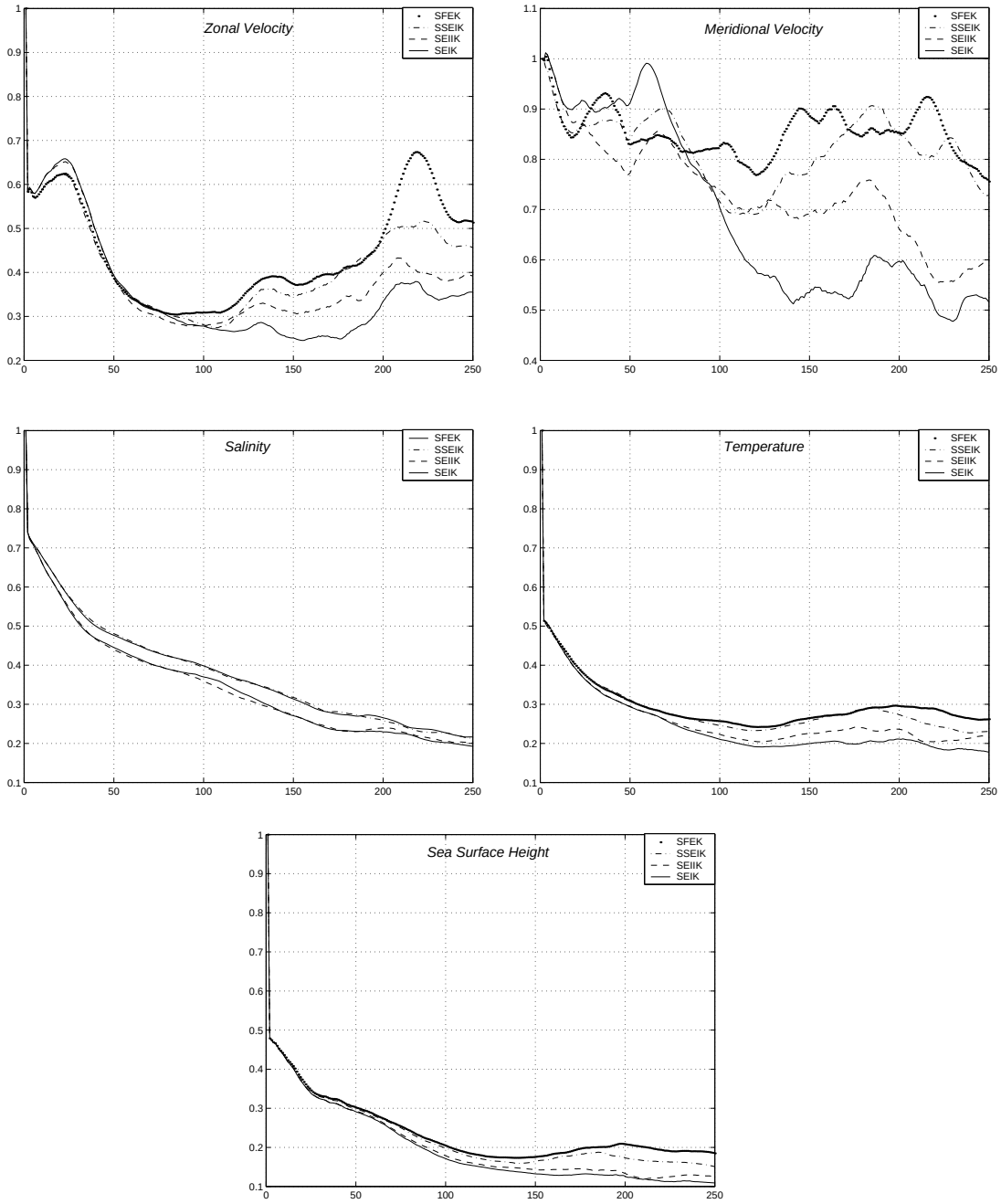

Figure 9: Evolution in time of the $RRMS$ for the SEIK, SFEK, SSEIK and SIEIK filters.

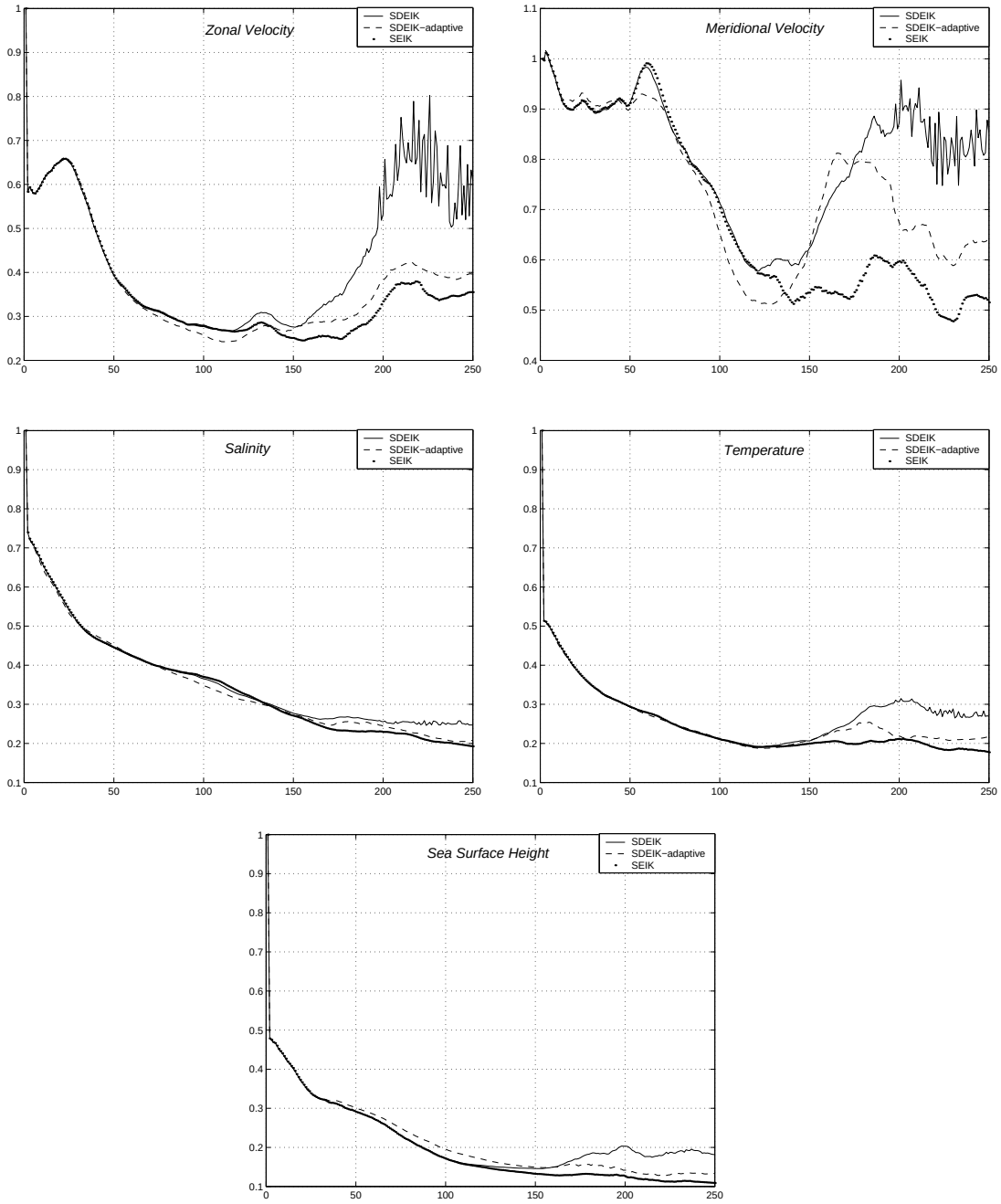

Figure 10: Evolution in time of the $RRMS$ for the SDEIK filter with and without adaptive tuning schemes and the SEIK filter.

with the adaptive tuning correction basis evolution scheme (presented in section 4) in order to show the usefulness of this scheme.

- *Adaptive tuning of the forgetting factor*

We discuss here the results of several experiments conducted to study the sensibility of our filters with respect to the forgetting factor ρ and to test the usefulness of the adaptive tuning scheme on ρ described in section 4. Since one can expect that the effects of the forgetting factor on different degraded SEIK filters are quite similar, we have only conduct experiment with the SFEK filter to save the computation cost. Therefore, we consider, on the one hand a fixed forgetting factor with three different values 1, 0.8 and 0.6 and on the other hand, a variable forgetting factor which takes value 1 or 0.6 according to the relative magnitudes of the short-term and long-term prediction error s_k and l_k. The initial values s_0 and l_0 were taken as $\|Y_0^o - H_k X^f(t_0)\|^2$ to make sure that ρ takes the value 0.6 during early assimilation period. The values of the constants α and β were chosen as 0.95 and 0.9 respectively.

Figure 11 shows the $RRMS$ error for these experiments: as expected, the SFEK filter diverges for $\rho = 1$ when model unstability appears. For $\rho = 0.8$, the SFEK performs relatively well but its results are not as good as for $\rho = 1$ in the stable period. Finally, the results of this filter are improved in the unstable period for $\rho = 0.6$, however its performance degraded in the stable period. We conclude from these experiments that the more the value of ρ is near to 1 the more the SFEK performs well in the stable period but we observe the opposite phenomena in the unstable period (under some limit on the minimum value of ρ). This confirms our argument on how to adapt to adapt the forgetting factor ρ. Furthermore, these results show the efficiency of our adaptive tuning scheme of the forgetting factor and, as can be seen form Figure 12, of the detection of the unstable periods.

In other assimilation experiments we study the usefulness of a variable forgetting factor on the SSEIK, the SIEIK and the SDEIK filters under the same previous setting. The results for the SSEIK filter are plotted in Figure 13. It can be seen that the performance of the SSEIK filter is significantly enhanced, particularly in the unstable period. A similar, but not as significant, improvement has been observed on the SIEIK filter. However, this scheme has no significant effect on the SDEIK filter.

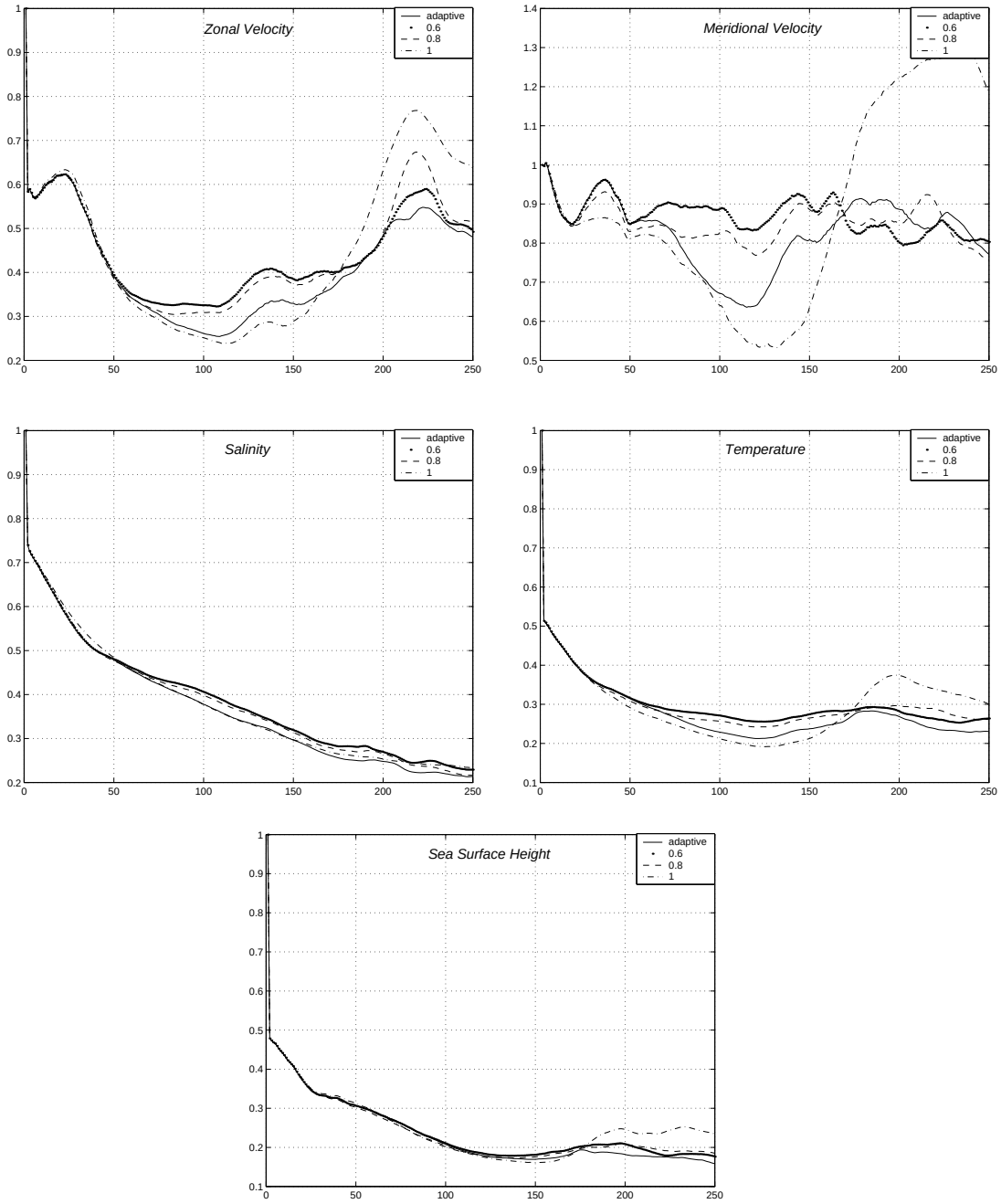

Figure 11: Evolution in time of the $RRMS$ for the SFEK filter with different values of the forgetting factor and with a variable forgetting factor.

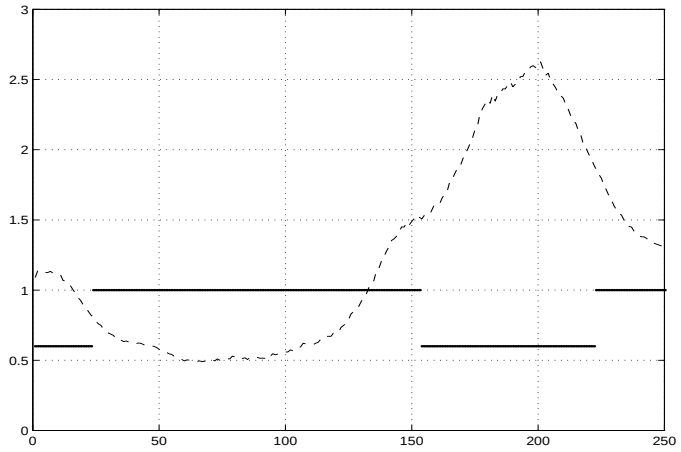

Figure 12: Evolution of the forgetting factor (solid line) and the relative variation of the state vector (dotted line).

• *Adaptive tuning of the correction basis evolution*

To test the relevance of the adaptive tuning scheme of the correction basis L_k evolution, we first compare the performance of the SIEIK filter, with and without this adaptation scheme, in the same situation as before. We chosen to let the correction basis L_k evolve once every 4 filtering steps and the forgetting factor was adapted taking the value 1 and 0.8. Note that we have increased the second value of because there is no need to use a small forgetting factor when the correction basis also evolves as in the SEIK filter, since the last is sufficiently stable during the unstable period. It can bee seen from Figure 14 that the adaptive tuning of the evolution of L_k noticeably improved the performance of the SIEIK filter.

The same previous set up has been used in experiments with the SDEIK, SFEK and the SSEIK filters. In Figure 10, one can clearly see by comparing the results of the SDEIK filter with and without this adaptation scheme that this filter was completely stabilized in the first case. Concerning the SFEK and the SSEIK filter and particularly for the last one, this adaptation scheme has made no significant improvement. This can be explained by the fact that the convergence of the correction basis towards the amplification error directions was very slow during the unstable period because of the last value of L_k.

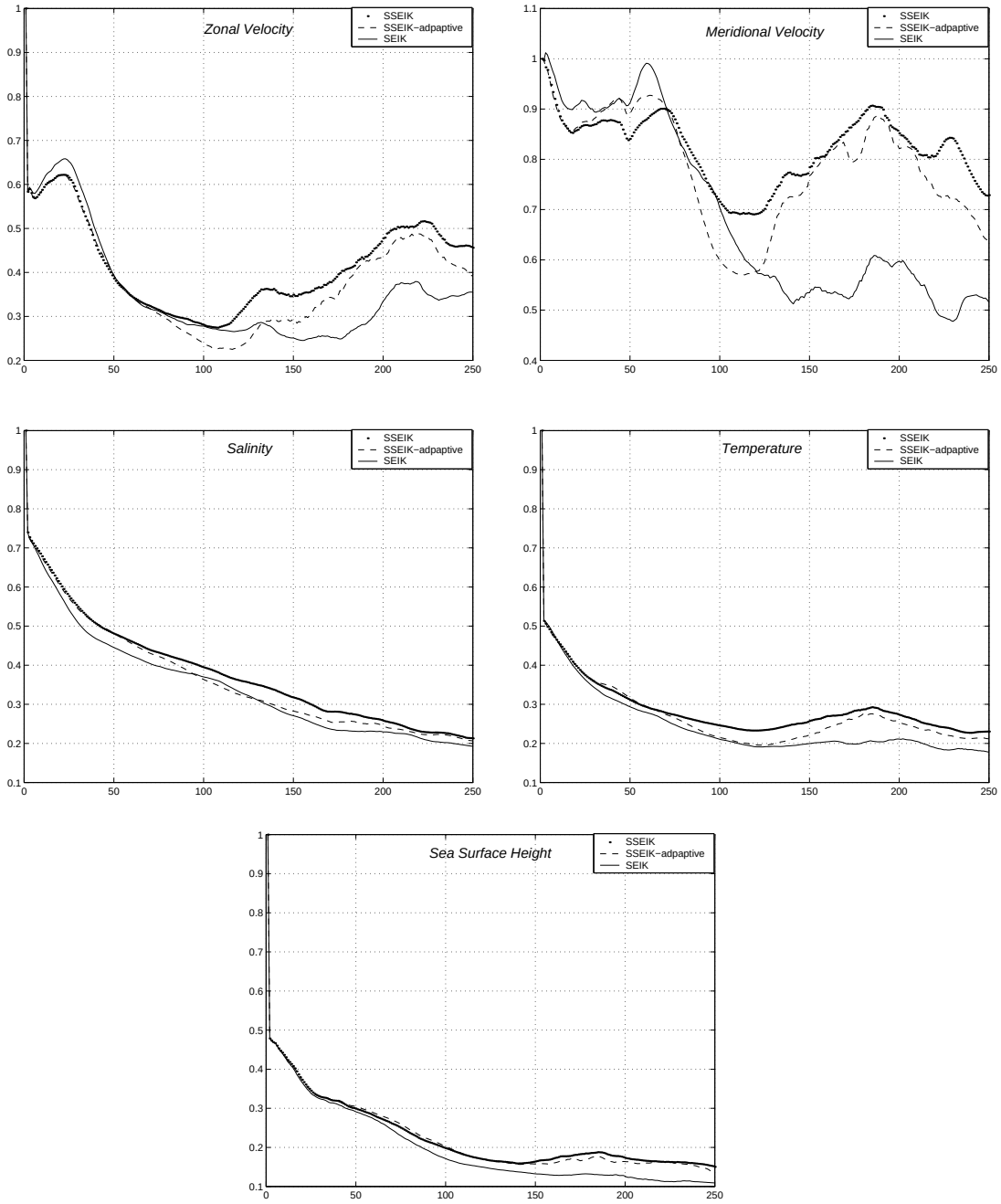

Figure 13: Evolution in time of the $RRMS$ for the SSEIK filter with and without adaption of the forgetting factor and the SEIK filter.

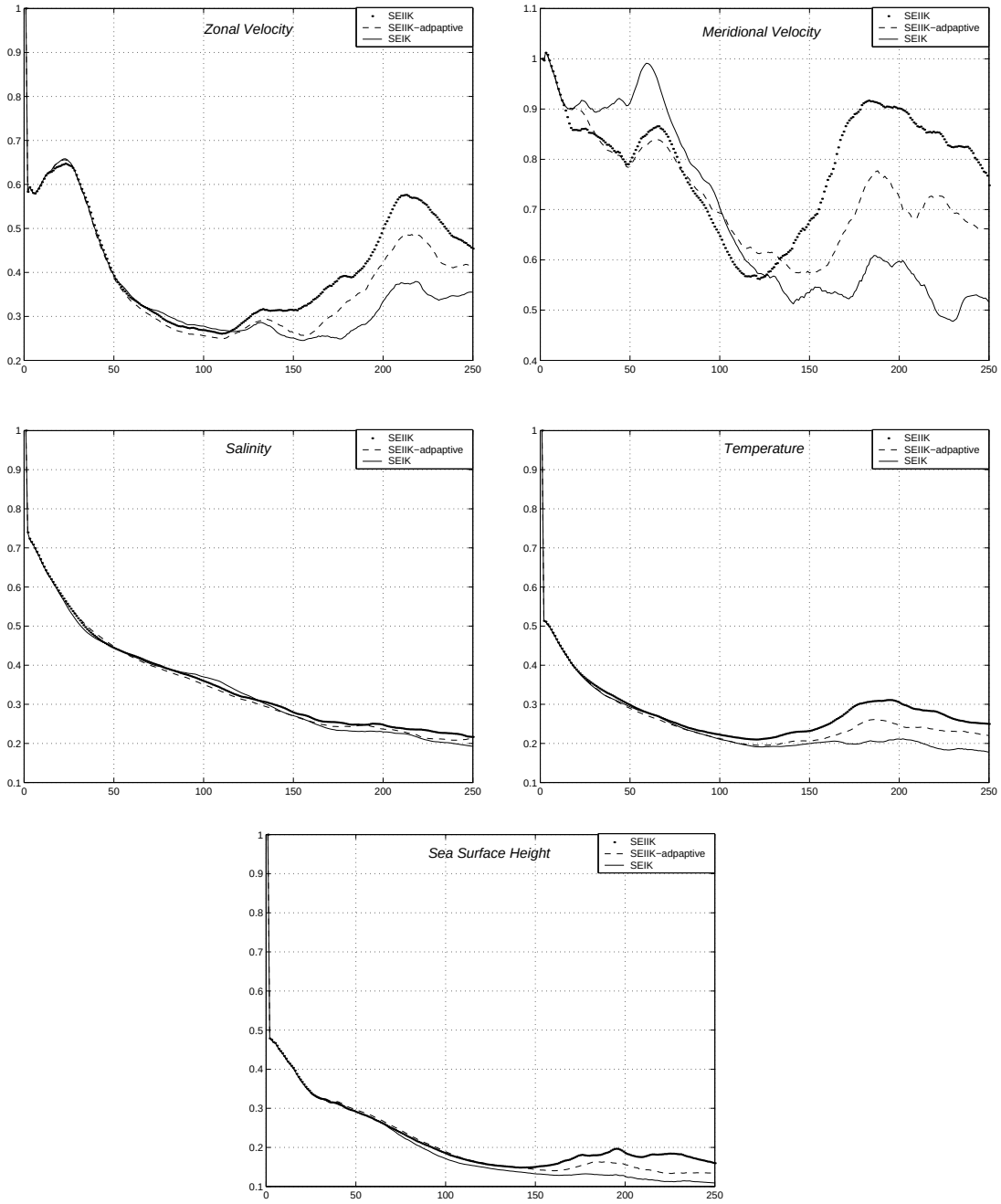

Figure 14: Evolution in time of the $RRMS$ for the SIEIK filter with and without adaptive tuning schemes and the SEIK filter.

6 Conclusions

New data assimilation schemes that derived from SEEK and SEIK filters have been developed and discussed. The motivation was essentially to reduce the cost of the SEEK and SEIK filters. Our approach was to simplify the way the evolution of the correction basis, which is the most expensive part of these filters. To deal with model unstabilities, we have proposed two adaptive schemes. The first consists in letting the correction basis evolves as in the SEIK filter during the unstable periods. The second scheme is to consider a variable forgetting factor. Moreover, a method to detect periods of unstability was suggested. It essentially consists of tracking the filter state by computing an instantaneous and a long-term prediction error norm. Finally, a series of twin experiments was conducted to assess the feasibilities of the new filters and to evaluate their performances in comparison with SEIK. Our main conclusions are as follows:

1- When model is stable, the degraded SEIK filters perform nearly as well as the SEIK filter, but can be 2 to 10 times faster. When model unstabilities appear, the assumptions on which the degraded SEIK filters have been constructed are no more justified and their performances degrade.

2- Without any adaptive scheme, comparison between all degraded SEIK filters shows the superiority of the SIEIK filter. With a very low cost, the SSEIK filter is well-behaved but only on one condition: the value of the forgetting factor is well tuned. Concerning the unstability of the SDEIK filter, one can remedy to this by combining this filter with the SEIK filter. The resulting filter seems to be very effective in practice. The performance of the SFEK filter is relatively poor which is understandable, however, it can be used in a preliminary study to get some idea for the tuning of the parameters of the SEIK filter and its variants, because of its very low cost.

3- By tracking the prevision errors one can obtain informations about the filter state and then adapt the filter parameters to the present situation.

4- Adaptive tuning of the forgetting factor considerably enhances the performance of all degraded SEIK filters. Moreover, its very low-cost makes it particularly attractive.

5- In most cases, and especially with the SDEIK filter, adaptive tuning of the evolution of the correction basis is useful; in few cases, it makes no significant improvement.

In twin experiments, our degraded SEIK filters was found to be fairly effective in assimilating of surface-only pseudo-altimeter data. Further works will consider a more realistic situations, like the addition of the model error or the use of a more realistic observations (according to satellite tracks and real data from satellite). However, these preliminary twin experiments applications were a necessary steps before realistic applications and provide us with encouraging as regard to that purpose.

A Drawing a random orthogonal matrix

We present here an algorithm to generate a uniform orthogonal matrix Ω with r columns orthonormal in $\mathbb{R}^{r+1}$ and orthogonal to $(1,\ldots,1)^T$ (see *Pham* [23] for more details). In order to do this, we will construct an iterative sequence of orthogonal matrix Ω_l, for l varies from 1 to r, as follows

1- Initialization: Take $\Omega_1 = w_{1,1}$ where $w_{1,1}$ is a random variable taking value 1 or -1 with a probability $\frac{1}{2}$.

2- Iteration: For $l = 1,\ldots,r$, we compute Ω_l from Ω_{l-1} with the formula

$$\Omega_l = \begin{pmatrix} & w_{l,1} \\ H(w_l)\Omega_{l-1} & \vdots \\ & w_{l,l} \end{pmatrix}, \tag{55}$$

where $w_l = (w_{l,1},\ldots,w_{l,l})^T$ is a random vector distributed uniformly on the unit sphere of $\mathbb{R}^l$ and $H(w_l)$ is the Householder matrix associated to the vector w_l, namely

$$H(w_l) = \begin{pmatrix} 1 & \ldots & 0 \\ \vdots & \ddots & \vdots \\ 0 & \ldots & 1 \\ 0 & \ldots & 0 \end{pmatrix} - \frac{1}{|w_{l,l}|+1} \begin{pmatrix} w_{l,1} \\ \vdots \\ w_{l,l-1} \\ w_{l,l} + sign(w_{l,l}) \end{pmatrix} (w_{l,l},\ldots,w_{l,l-1}) \ .$$

Note that the columns of $H(w_l)$ are orthonormal and orthogonal with the vector w_l. One can then show that the matrices $\Omega_l, l = 1,\ldots,r$ are random orthogonal matrices distributed uniformly. Finally, to obtain Ω, just multiply Ω_r the Householder matrix associated to the normed vector $\frac{1}{\sqrt{r+1}}(1,\ldots,1)^T$.

B Summary of the Filters costs

This table provides approximations of the cost of all the filters implemented in section 5.3 with respect to the SEIK's cost. Just recall here that the cost of the SEIK filter is slightly higher than

$$(r+1) \times \{model\ cost\}, \tag{56}$$

where r is the correction basis dimension.

Filters	*Cost with respect to the SEIK*
$SFEK$	$(1/30) * \{cost\ of\ SEIK\}$
$SFEK - adaptive$	$(1/30) * \{cost\ of\ SEIK\}$
$SSEIK$	$(1/15) * \{cost\ of\ SEIK\}$
$SSEIK - adaptive$	$(1/15) * \{cost\ of\ SEIK\}$
$SIEIK(1/4)$	$(1/4) * \{cost\ of\ SEIK\}$
$SIEIK - adaptive$	$(2/5) * \{cost\ of\ SEIK\}$
$SIEIK(1/2)$	$(1/2) * \{cost\ of\ SEIK\}$
$SDEIK$	$(1/2) * \{cost\ of\ SEIK\}$
$SDEIK - adaptive$	$(3/5) * \{cost\ of\ SEIK\}$

References

[1] Arakawa A. (1972): Design of the UCLA general circulation model. Numerical integration of weather and climate. *Dept. of Meteorology*, University of California, **Rep. 7**, 116 pp.

[2] Astrom K.J. and B. Wittenmark (1989): Adaptive control. *Addison-Wesley publishing company*.

[3] Blanke B. and P. Delecluse (1993): Variability of the tropical Atlantic ocean simulated by a general circulation model with two different mixed layer physics. *J. Phys. Oceanogr.*, **23**, 1363-1388.

[4] Brasseur P., J. Ballabrera-Poy and J. Verron (1999): Assimilation of altimetric observations in a primitive equation model of the gulf stream using a singular evolutive extended Kalman filter. *J. Mar. Systems*, **22**(4), 269-294.

[5] Cane M.A., A. Kaplan, R.N. Miller, B. Tang, E.C. Hackert and A.J. Busalacchi (1995): Mapping tropical Pacific sea level: data assimilation via a reduced state Kalman filter. *J. Geophys. Res.*, **vol.101**, no.C10, 599-617.

[6] Cohn S.E. and R. Tolding (1996): Approximate Kalman filters for stable and unstable dynamics. *J. Meteor. Soc. Japan*, **74**, 63-75.

[7] Dee D.P. (1990): Simplification of the Kalman filter for meteorological data assimilation. *Quart. J. Roy. Meteor. Soc.*, **vol.117**, 365-384.

[8] Evensen G. (1994): Sequential data assimilation with a nonlinear quasi-geostrophic model using Monte Carlo methods to forecast error statistics. *J. Geophys. Res.*, **vol.99**, no.C5, 10143-10162.

[9] Evensen G. (1992): Using the extended Kalman filter with a multilayer quasi-geostrophic ocean model. *J. Geophysical Research*, **vol.97**, no.C11, 17905-17924.

[10] Farrell B.F. (1989): Optimal excitation of baroclinic waves. *J. Geophys. Res. Oceans*, **100**, 6777-6793.

[11] Fukumori I. and P. Malanotte-Rizzoli (1995): An approximate Kalman filter for ocean data assimilation: an example with an idealized gulf stream model. *J. Geophys. Res.*, **100**(C4), 6777-6793.

[12] Gauthier P., P. Courtier and P. Moll (1993): Assimilation of simulated wind Lidar data with a Kalman filter. *Mon. Wea. Rev*, **vol. 121**, 1803-1820.

[13] Ghil M. and P. Malanotte-Rizzoli (1991): Data assimilation in meteorology and oceanography. *Adv. Geophys.*, **33**, 141-266.

[14] Hoang H.S., P. De Mey, O. Tallagrand and R. Baraille (1995): Assimilation of altimeter data in multilayer quasi-geostrophic model by simple nonlinear adaptive filter. *Proc. Internat. Symposium Assimilation Obser. Meteo. Oceano.*, 521-526, Tokyo, Japan.

[15] Ide K., A.F. Bennett, P. Courtier, M. Ghil and A.C. Lorenc (1997): Unified notation for data assimilation: operational, sequential and variational. *J. Met. Soc.*, Japan, 75(1B), 181-189.

[16] Jazwinski A.H. (1970): Stochastic processes and filtering theory. *Academic Presse*, New York.

[17] Levitus S. (1982): Climatological atlas of the world ocean. *Geophysical fluid dynamics laboratory*, Princeton.

[18] Madec G., P. Delecluse, M. Imbard and C. Levy (1997): Ocean General Circulation Model Reference Manual. *Technical report*, University Pierre and Marie Curie, Paris VI.

[19] Moore A.M. and B.F. Farrell (1994): Using adjoint models for stability and predictability analysis. *Data assimilation: Tools for modeling the ocean in a global change perspective*, P.P. Brasseur and J.C.J. Nihoul, Eds, NATO ASI Series, **vol. 19**, 253 pp.

[20] Pham D.T. (1998): Stochastic methods for sequential data assimilation in strongly nonlinear systems. *Rapport de recherche*, **N° 3597**, INRIA.

[21] Pham D.T., J. Verron and L. Gourdeau (1998): Singular evolutive Kalman filters for data assimilation in oceanography. *C. R. Acad. sci. Paris*, **vol. 326**, 255-260.

[22] Pham D.T., J. Verron and M.C. Roubaud (1997): Singular evolutive Kalman filter with EOF initialization for data assimilation in oceanography. *J. Mar. Syst.*, **vol.** 16, 323-340.

[23] Pham D.T. (1996): A singular evolutive interpolated Kalman filter for data assimilation in oceanography. *Technical report*, **RT 163**, Projet IDOPT CNRS-INRIA.

[24] Sorenson H.W. and J.E. Sacks (1971): Recursive fading memory filtering. *Information Sciences*, **3**, 101-119.

[25] Trefethen L.N., A.E. Trefethen, S.C. Reddy and T.A. Driscoll (1993): Hydrodynamic stability without eigenvalues. *Science*, **261**, 571-584.

[26] Verron J., L. Gourdeau, D.T. Pham, R. Murtugudde and A.J. Busalacchi (1998): An extended Kalman filter to assimilate satellite altimeter data into a non-linear numerical model of the tropical pacific: method and validation. *J. Geophysical Research*, **vol. 104**, C3, 5441-5458.

Unit´e de recherche INRIA Lorraine, Technopôle de Nancy-Brabois, Campus scientifique,
615 rue du Jardin Botanique, BP 101, 54600 VILLERS LÈS NANCY
Unit´e de recherche INRIA Rennes, Irisa, Campus universitaire de Beaulieu, 35042 RENNES Cedex
Unit´e de recherche INRIA Rhône-Alpes, 655, avenue de l'Europe, 38330 MONTBONNOT ST MARTIN
Unit´e de recherche INRIA Rocquencourt, Domaine de Voluceau, Rocquencourt, BP 105, 78153 LE CHESNAY Cedex
Unit´e de recherche INRIA Sophia-Antipolis, 2004 route des Lucioles, BP 93, 06902 SOPHIA-ANTIPOLIS Cedex

Éditeur
INRIA, Domaine de Voluceau, Rocquencourt, BP 105, 78153 LE CHESNAY Cedex (France)
http://www.inria.fr
ISSN 0249-6399